AD-A137 362 AN EVALUATION OF 700 MB AIRCRAFT RECONNAISSANCE DATA 1/1
FOR SELECTED NORTHWEST PACIFIC TROPICAL CYCLONES(U)
NAVAL POSTGRADUATE SCHOOL MONTEREY CA G M DUNNAVAN
UNCLASSIFIED SEP 83 F/G 4/2 NL

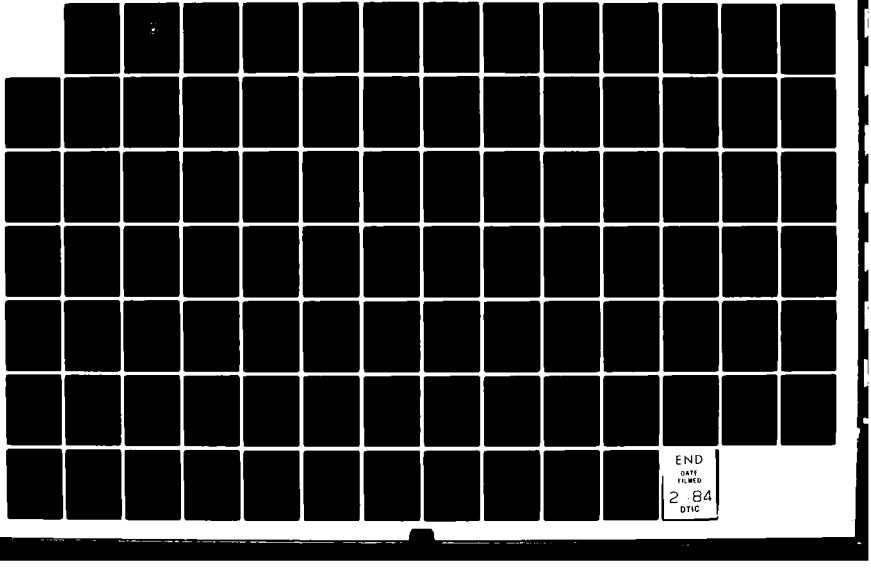

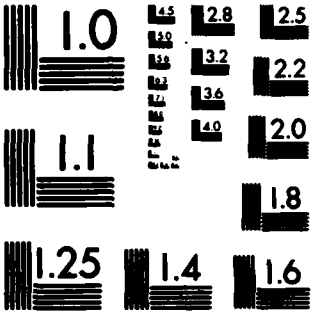


MICROCOPY RESOLUTION TEST CHART
NATIONAL BUREAU OF STANDARDS-1963-A

# NAVAL POSTGRADUATE SCHOOL
## Monterey, California

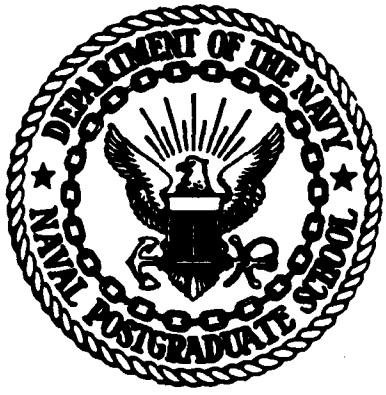




# THESIS

AN EVALUATION OF 700 MB AIRCRAFT RECONNAISSANCE DATA FOR SELECTED NORTHWEST PACIFIC TROPICAL CYCLONES

by

George Milton Dunnavan

Thesis Advisor: R. L. Elsberry

Approved for public release; distribution unlimited.

SECURITY CLASSIFICATION OF THIS PAGE (When Data Entered)

| REPORT DOCUMENTATION PAGE | READ INSTRUCTIONS BEFORE COMPLETING FORM |
|---|---|
| 1. REPORT NUMBER | 2. GOVT ACCESSION NO. AD-A137362 | 3. RECIPIENT'S CATALOG NUMBER |
| 4. TITLE (and Subtitle) An Evaluation of 700 mb Aircraft Reconnaissance Data for Selected Northwest Pacific Tropical Cyclones | 5. TYPE OF REPORT & PERIOD COVERED Master's Thesis; September 1983 |
| | 6. PERFORMING ORG. REPORT NUMBER |
| 7. AUTHOR(s) George Milton Dunnavan | 8. CONTRACT OR GRANT NUMBER(s) |
| 9. PERFORMING ORGANIZATION NAME AND ADDRESS Naval Postgraduate School Monterey, California 93943 | 10. PROGRAM ELEMENT, PROJECT, TASK AREA & WORK UNIT NUMBERS |
| 11. CONTROLLING OFFICE NAME AND ADDRESS Naval Postgraduate School Monterey, California 93943 | 12. REPORT DATE September 1983 |
| | 13. NUMBER OF PAGES 92 |
| 14. MONITORING AGENCY NAME & ADDRESS(if different from Controlling Office) | 15. SECURITY CLASS. (of this report) UNCLASSIFIED |
| | 15a. DECLASSIFICATION/DOWNGRADING SCHEDULE |

16. DISTRIBUTION STATEMENT (of this Report)

Approved for public release; distribution unlimited

17. DISTRIBUTION STATEMENT (of the abstract entered in Block 20, if different from Report)

18. SUPPLEMENTARY NOTES



19. KEY WORDS (Continue on reverse side if necessary and identify by block number)

Tropical cyclones
Typhoons
Hurricanes
Aircraft reconnaissance
Tropical cyclone intensity
Equivalant potential temperature
Moist static energy

20. ABSTRACT (Continue on reverse side if necessary and identify by block number)

The 700 mb aircraft reconnaissance data for 25 selected northwest Pacific tropical cyclones were analyzed and compared with similar data for Atlantic tropical cyclones. Correlations of observed winds and winds calculated from the height gradient indicated that the cyclostrophic equation provided a very good approximation of the observed winds, although the root mean square and bias errors suggested that a gradient wind

DD FORM 1 JAN 73 1473 EDITION OF 1 NOV 65 IS OBSOLETE
S/N 0102-LF-014-6601

SECURITY CLASSIFICATION OF THIS PAGE (When Data Entered)

expression was a slightly better estimate. A wind-radius relationship evaluated by Shea and Gray (1972) for Atlantic cyclones was shown to apply very well for this data set also. Based on the surface pressure-equivalant potential temperature relationship noted by Malkus and Riehl (1960), it is proposed that periods of rapid/explosive deepening are related to the inward transport to the eyewall of "pulses" of high equivalent potential temperature air. The evaluation of the aircraft reconnaissance data from four super typhoons suggests, but does not provide conclusive proof, that such pulses do exist.

Approved for public release; distribution unlimited

# An Evaluation of 700 mb Aircraft Reconnaissance Data for Selected Northwest Pacific Tropical Cyclones

by

George M. Dunnavan
Lieutenant, United States Navy
B.S., University of Washington, 1975

Submitted in partial fulfillment of the
requirements for the degree of

MASTER OF SCIENCE IN METEOROLOGY AND OCEANOGRAPHY

from the

NAVAL POSTGRADUATE SCHOOL
September 1983

Author: _____

Approved by: _____ Thesis Advisor

_____ Second Reader

_____ Chairman, Department of Meteorology

_____ Dean of Science and Engineering

## ABSTRACT

The 700 mb aircraft reconnaissance data for 25 selected northwest Pacific tropical cyclones were analyzed and compared with similar data for Atlantic tropical cyclones. Correlations of observed winds and winds calculated from the height gradient indicated that the cyclostrophic equation provided a very good approximation of the observed winds, although the root mean square and bias errors suggested that a gradient wind expression was a slightly better estimate. A wind-radius relationship evaluated by Shea and Gray (1972) for Atlantic cyclones was shown to apply very well for this data set also. Based on the surface pressure-equivalent potential temperature relationship noted by Malkus and Riehl (1960), it is proposed that periods of rapid/explosive deepening are related to the inward transport to the eyewall of "pulses" of high equivalent potential temperature air. The evaluation of the aircraft reconnaissance data from four super typhoons suggests, but does not provide conclusive proof, that such pulses do exist.

TABLE OF CONTENTS

LIST OF FIGURES

## LIST OF TABLES

## ACKNOWLEDGEMENT

The author wishes to thank Professor R. L. Elsberry for his thorough evaluation of this manuscript. His knowledge of research techniques and command of the English language were invaluable. The comments and suggestions of Dr. Johnny Chan provided the author with much insight into the most current theories of tropical cyclone development and were likewise greatly appreciated. Special thanks are due Dr. Ted Tsui and AGCM D. Ales of the Naval Environmental Prediction Research Facility (NEPRF), who obtained the tropical cyclone data for this study, and also to Marion Marks who coded the raw data for computer evaluation.

# I. INTRODUCTION

To define the structure and dynamics of any atmospheric phenomenon, it is necessary to obtain observational data, both horizontally and vertically, in the vicinity of the phenomenon. The data collected, e.g., temperature, humidity, height of pressure surface, wind direction and speed, can be used to construct a model of the phenomenon. Theories which have been developed to describe the phenomenon in physical or mathematical terms can then be tested against the "ground truth" of the observational model. Routine meteorological observations from pilot balloons, rawinsondes, aircraft and, more recently, satellite sounders, have become available only within the latter half of this century. Surface observations are generally clustered near land masses. Quality upper air data over oceans are confined to the few island reporting stations and along airline routes and, therefore, usually do not adequately describe the significant weather activity over large areas of the oceans.

One area of research which has suffered greatly from the scarcity of high quality observational data is the study of tropical cyclones. Data collected in the vicinity of

tropical cyclones are sparse for two reasons: 1) tropical cyclones tend to be confined for most of their lives to tropical ocean areas, where the number of upper air observing sites is limited; and 2) aircraft and ships tend to avoid tropical cyclones for safety considerations.

Due to these constraints on the quantity of tropical cyclone data, studies using these data are necessarily of two basic types: the "case study" method and the "composite method". The case study approach involves the study of the observations associated with single tropical cyclones (e.g., La Seur and Hawkins, 1963). This technique can only be employed if a large amount of data has been collected (e.g., via special aircraft reconnaissance) because the normal data coverage is generally too sparse to describe the tropical cyclone structure adequately. The composite method may be divided into three subgroups. The "rawinsonde composite" technique involves the combination of a large number of rawinsonde observations collected from different storms over a long time period (Jordan, 1952; Frank, 1977). The "composite aircraft reconnaissance data" method involves the evaluation of a large number of aircraft observations in the vicinity of many tropical cyclones (Shea and Gray, 1973).

The third method combines aircraft and rawinsonde data through a compositing technique. The rawinsonde composite studies have provided valuable insight into the large scale structure of the tropical cyclone and its environment. However, inferences concerning the structure close to the center of the system, e.g. within 100 NM (nautical miles), become tenuous because of the smaller data base available. Upper-air soundings near the center of tropical cyclones are rare for two reasons. Tropical cyclones form over tropical oceans away from rawinsonde sites, and it is very difficult to launch rawinsondes during the adverse weather conditions associated with mature tropical cyclones.

On the other hand, reconnaissance aircraft have provided routine observations of the tropical cyclone circulation during various stages of its development. The major drawback to aircraft observations is that they are taken at only a small number of pressure levels (usually only one), and thus do not provide the vertical structure information which a rawinsonde does. Still, much information concerning the central structure can be gleaned from the large amount of aircraft data which is available from many cyclones.

This thesis presents analyses of 700 mb aircraft reconnaissance data for 25 selected tropical cyclones which occurred in the northwest Pacific between 1978 and 1981. The first goal of this study was to determine if the meteorological observations obtained by operational reconnaissance aircraft (whose primary mission is forecast support) are of sufficiently high quality to provide tropical cyclone structure information which is consistent with the information provided by the more sophisticated research aircraft. Second, an attempt was made to determine, from the 700 mb aircraft data, if a relationship exists between the arrival of high equivalent potential temperature air near the eyewall and a subsequent drop in central surface pressure.

## II. RECONNAISSANCE AIRCRAFT TROPICAL CYCLONE DATA

### A. BACKGROUND

Early aircraft reconnaissance (T & WA, Inc, 1945; Wexler and Wood, 1945) was conducted primarily to determine whether it was possible for an aircraft to penetrate safely through the center of a mature tropical cyclone. Observations during these flights were mainly visual, but they did provide new information concerning the large-scale dynamic and thermodynamic processes which take place near the center of a tropical cyclone. For example, early reconnaissance flights discovered the existence of a narrow band of ascending air near the cyclone center, "the eyewall", with generally descending air (except in the vicinity of the rainbands) outside of this area (Wexler and Wood, 1945). Prior to these obeservations, it was thought that ascending air should exist over the entire area encompassed by the cyclone, with descending air only within the eye.

By the late 1940's, aircraft reconnaissance to support tropical cyclone forecast centers was being routinely conducted by the U.S. Navy and Air Force in the Atlantic and

the northwest Pacific Oceans. Although these flights were operational in nature, it was often possible to gather research data. Simpson (1952, 1954) and Simpson and Starrett (1955) performed the first extensive evaluation of aircraft reconnaissance data from operational and research flights into both Atlantic and northwest Pacific tropical cyclones. Information provided by these studies expanded and, in some cases, altered the existing theories of the horizontal and vertical structure of the tropical cyclone temperature and wind fields, pressure gradients and associated cloud features. With the advent of specially equipped tropical cyclone research aircraft in 1955, it was possible to increase both the quantity and quality of the data collected. This advancement was crucial for the detailed study of the near-eye structure as well as the wind, pressure, temperature and dewpoint fields (La Seur and Hawkins, 1963).

The most complete study to date of the tropical cyclone's inner core region was accomplished by Shea and Gray (1973), who composited 13 years of research aircraft reconnaissance data for tropical cyclones in the west Atlantic Ocean. The composite of this large amount of data allowed the documentation of subtle wind and temperature

asymmetries. The variability among the individual cyclones was also demonstrated.

Studies of aircraft reconnaissance data from operational and research flights have also provided the operational forecaster with some useful tools. These include: a technique for estimating central sea level pressure from aircraft observations (Jordan, 1958); a proposed method for the determination of tropical cyclone intensity through upper-tropospheric aircraft reconnaissance (Gray, 1979b); and a technique for forecasting intense tropical cyclones using aircraft-provided temperature and dew point data (Dunnavan, 1981).

## B. NORTHWEST PACIFIC AIRCRAFT DATA COLLECTION

Tropical cyclone aircraft reconnaissance in the northwest Pacific is conducted by the 54th Weather Reconnaissance squadron of the United States Air Force using WC-130 aircraft. Since 1978, the Aircraft Reconnaissance Weather Officer (ARWO) on each reconnaissance mission has prepared "peripheral data" messages which are relayed to the forecasters at the Joint Typhoon Warning Center (JTWC) in Guam via teletype. The peripheral data message contains the position of the tropical cyclone's 700 mb center, the 700 mb

height, temperature and dew point at that center; and the 700 mb height, temperature, dew point and flight level wind at 30, 60, 90 and 120 NM from the cyclone center for both an inbound and an outbound flight leg. Except in areas of restricted airspace, the inbound and outbound legs are in different (usually opposite) quadrants of the cyclone. It has been the policy of the JTWC to request aircraft reconnaissance to support at least two of the four daily tropical cyclone warnings, when logistically possible. Thus, 700 mb peripheral data, observed at intervals of 12 h (hours) or less, has been collected for many northwest Pacific tropical cyclones from 1978 to the present.

The 700 mb height data were obtained using an AN/APN-42A Radar Altimeter (or as a backup, either an SCR-718 or APN-133 Radio Altimeter), together with a Garrett Airsearch Digital Pressure Encoder (or as a backup, an AIMS Counter-drum pointer Aneroid Pressure Altimeter). The radar or radio altimeter provided the absolute altitude of the aircraft and the pressure encoder (or altimeter) provided the pressure altitude. A series of calculations and corrections was employed to reduce these two measurements to a 700 mb height value (Henderson, 1980). The accuracy of a 700 mb

height determined this way is about 20 m (Det 4, Air Weather Service, 1980, Typhoon Duty Officer Brief).

The 700 mb temperatures were measured by a Rosemount AN/AMQ-28 Total Temperature System. This device employs a resistance element in an external probe which is positioned to reduce frictional effects. It is accurate to within $1^{o}$C (Henderson, 1980).

The 700 mb dew point temperatures were measured by a Cambridge Systems AN/AMQ-34 Aircraft Hygrometer. This instrument essentially measures the temperature of a mirror which has been cooled to the point where condensation forms. The device is accurate to within $1^{o}$ C for temperatures above $0^{o}$ C (Henderson, 1980).

The flight level winds (i.e. 700 mb) were determined using a one-minute average from a Doppler radar. Measured wind directions are accurate to within 5 degrees and speeds to within 5 kt (knots). It should be noted that Doppler attenuation in heavy precipitation could produce spuriously low wind speed values (Det 4, Air Weather Service, 1980, Typhoon Duty Officer Brief). Wind speeds were not reported if it was obvious to the observer that extreme attenuation had occurred. However, small reductions in wind speed due

to attenuation were generally not detectable, and therefore were a source of error in the data base.

## C. TROPICAL CYCLONES USED FOR THIS STUDY

It was decided that only those tropical cyclones which transited the Philippine Sea east of the Philippine Islands, west of the Island of Guam and south of Japan would be considered for this study for the following reasons. By analyzing tropical cyclones which existed in the same general area, but reached different intensities, it was hoped that any geographic dependence on intensification would be reduced. Climatology indicates that the overwhelming majority of northwest Pacific tropical cyclones pass through this area (Joint Typhoon Warning Center, 1979-1982). Also, most tropical cyclones which reach super-typhoon strength, or undergo a period of rapid intensification, do so in this region (Holliday and Thompson, 1979). Rawinsonde sites are sparse in this part of the Pacific, so it was necessary for the JTWC to request extensive aircraft reconnaissance for cyclones in this area. This region is also equidistant from the reconnaissance aircraft launch and recovery sites at Clarke Air Base in the Philippine Islands, Yokota Air Base in Japan, Andersen Air Force Base on Guam, and Kadena Air

Base on Okinawa. Thus, the aircraft have long on-station times which permit the collection of large amounts of data in the vicinity of cyclones in this area. Reconnaissance aircraft observations for storms outside of the region were excluded from this study.

TABLE I

List of Tropical Cyclones With Peripheral Data

# ST = super typhoon, TY = typhoon, TS = tropical storm

| Year | Month | | Cyclone Name | Maximum Wind (kt) | Min Pressure (mb) | No. of Radial Legs |
|---|---|---|---|---|---|---|
| 1981 | Aug | TY# | Thad | 85 | 965 | 34 |
| 1981 | Sep | ST | Elsie | 150 | 893 | 38 |
| 1981 | Nov | TY | Hazen | 100 | 956 | 32 |
| 1981 | Nov | ST | Irma | 135 | 902 | 32 |
| 1981 | Nov | TS | Jeff | 35 | 999 | 6 |
| 1981 | Dec | TY | Kit | 115 | 924 | 60 |
| 1980 | May | TY | Dom | 90 | 956 | 14 |
| 1980 | May | TY | Ellen | 110 | 931 | 60 |
| 1980 | Jul | TS | Ida | 60 | 980 | 18 |
| 1980 | Jul | TY | Joe | 105 | 940 | 22 |
| 1980 | Jul | ST | Kim | 130 | 908 | 40 |
| 1980 | Oct | TY | Betty | 120 | 928 | 44 |
| 1979 | Jan | TY | Alice | 110 | 930 | 76 |
| 1979 | Mar | TY | Bess | 90 | 958 | 30 |
| 1979 | Jul | TS | Faye | 40 | 998 | 10 |
| 1979 | Jul | ST | Hope | 130 | 898 | 6 |
| 1979 | Aug | TY | Irving | 90 | 954 | 34 |
| 1979 | Aug | ST | Judy | 135 | 887 | 52 |
| 1979 | Sep | TY | Owen | 110 | 918 | 58 |
| 1979 | Oct | ST | Tip | 165 | 870 | 102 |
| 1979 | Nov | ST | Vera | 140 | 915 | 28 |
| 1979 | Dec | TY | Abby | 110 | 951 | 64 |
| 1978 | Jul | TY | Trix | 70 | 967 | 44 |
| 1978 | Oct | ST | Rita | 155 | 878 | 58 |
| 1978 | Nov | TY | Viola | 125 | 911 | 40 |

TOTAL RADIAL LEGS = 1002

The geographic constraints established above allowed the selection of 25 tropical cyclones which developed between 1979 and 1981. All of the peripheral data for these 25

cyclones were obtained from the archives of the National Climate Center (Table I). This set included eight super typhoons (maximum sustained winds of 130 kt or greater), nine average typhoons (maximum sustained winds between 100 kt and 130 kt) and eight weaker tropical cyclones ( maximum winds less than 100 kt).

D. DATA PREPARATION

Copies of the peripheral data messages prepared by the ARWOs were obtained from the National Climate Center. The message format was sufficiently consistent from year to year to allow compiling of the data into a master file of all of the aircraft observations from the 25 tropical cyclones. The master file contained 4008 observations, each of which contained: the year, month, date and time of the observation, the cyclone name and number; the 700 mb height, temperature and dew point at the cyclone center; the 700 mb height, temperature, dew point and flight level wind speed and direction at the location; the location of the cyclone center (latitude and longitude); the location of the observation with respect to the cyclone center by quadrant and radial distance from the center (30, 60, 90, or 120 NM); a designation which indicated whether the cyclone ultimately

became a weak, typical or super typhoon; and an indication if the observation was made before the cyclone reached maximum intensity.

Eight consecutive lines represented one peripheral data message. That is, four inbound observations ( at 120, 90, 60, and 30 NM) in one quadrant, and four outbound observations ( at 30, 60, 90 and 120 NM) in another quadrant. To reduce the effects of cyclone movement and asymmetries in the dynamic and thermodynamic fields, a second data set was generated. This data set was composed of 2004 observations which represented the metecrological variables at 30, 60, 90 and 120 NM as determined by averaging the values obtained on the inbound leg and outbound leg at each radial distance for each penetration of the tropical cyclone.

## III. THE HORIZONTAL WIND STRUCTURE OF THE CYCLONES

After the aircraft data had been averaged as described in Chapter II and scanned for obvious errors, they were analyzed to determine if the wind observations satisfied gradient and/or cyclostrophic mass-wind balance. Also, a wind speed-radius relationship was evaluated and compared to a relationship noted by Hughes (1952), Malkus and Riehl (1960) and Shea and Gray (1972).

The evaluation of the observed winds involved three basic assumptions. First, it was assumed that the average of the wind speeds for the inbound and outbound legs at a radius was somewhat representative of the wind speed for the entire tropical cylcone at that radius and time. This assumption would have been stronger if it had been possible to average more than just two radial legs at a time. Secondly, it was assumed that the magnitude of the tangential wind could be approximated by the magnitude of the observed wind. This assumption is supported by the findings of Shea and Gray (1973), who determined that there was very weak azimuthally-averaged inflow or outflow at the

mid-levels (750, 650, 525 mb) from the radius of maximum winds (RMW) to at least 40 NM. This implies that the radial wind was either very small, or that the inward radial velocities occurred as often as the outward velocities. It was assumed that Shea and Gray's results could be applied to the 700 mb level and out to 120 NM. With a large data set, such as the one used in this study, the azimuthal averaging would tend to eliminate the radial wind component so that the observed wind would be a good approximation of the tangential wind. Finally, the mass-wind balance equations which were used in this study are valid for steady state situations only (i.e. the wind speed is not changing with time). Although the data represent tropical cyclones at all stages of development, it was believed that the large size of the data set would allow for an assumption of steady state conditions. This same assumption was also made by Shea and Gray (1973).

## A. THE MASS-WIND BALANCE

The gradient wind balance equation (Holton, 1979) can take the form:

$$\frac{V^2}{r} + fV = \frac{\partial \phi}{\partial r} \qquad (1)$$

where, V = tangential wind speed

r = radial distance from the center

f = Coriolis parameter

$\phi$ = geopotential height

Solving for V with the positive root yields:

$$V = -\frac{rf}{2} + \sqrt{\frac{r^2 f^2}{4} + r\frac{\partial \phi}{\partial r}} \qquad (2)$$

Because 700 mb height data were available at 0, 30, 60, 90 and 120 NM from the cyclone center, $\frac{\partial \phi}{\partial r}$ could be estimated at 30, 60, and 90 NM using a centered finite difference scheme. By using this approximation to the derivative, it was possible to calculate gradient wind speeds based on the latitude of the cyclone, the distance from the cyclone center and the 700 mb geopotential height gradient. These gradient wind speeds were then compared to the observed wind speeds (Table II).

The Coriolis parameter in the tropics is small, and the wind speeds associated with tropical cyclones can be high. As a consequence, a scaling of the individual terms in the gradient wind equation indicates that to a good approximation, this equation can be reduced to a cyclostrophic balance equation:

$$\frac{V^2}{r} = \frac{\partial \phi}{\partial r} \qquad (3)$$

or $$V = \sqrt{r \frac{\partial \phi}{\partial r}} \qquad (4)$$

Intuitively, this balance should be most applicable near the cyclone center where r is small and/or in the lower latitudes where the Coriolis parameter is small. These cyclostrophic winds were also compared to the observed winds at 30, 60 and 90 NM (Table II).

TABLE II

Correlation of Cyclostrophic/Gradient Wind and Observed Wind

| Balance Radius (NM) | Obs. Used | Corr. Coeff. | Regression equation % (winds in m/s) |
|---|---|---|---|
| "Ideal Case" | | 1.000 | y = 1.000 x + 0.0 |
| Gradient | | | |
| 30 | ALL | .782 | y = 1.075 x + 2.5 |
| | Lat LT 20 N # | .798 | y = 1.116 x + 2.3 |
| | Lat GT 20 N * | .736 | y = .922 x + 4.4 |
| 60 | ALL | .812 | y = 1.011 x + 2.1 |
| | Lat LT 20 N | .809 | y = 1.021 x + 1.7 |
| | Lat GT 20 N | .805 | y = .960 x + 3.9 |
| 90 | ALL | .800 | y = .947 x + 2.5 |
| | Lat LT 20 N | .824 | y = .988 x + 1.4 |
| | Lat GT 20 N | .685 | y = .796 x + 7.0 |
| Cyclostrophic | | | |
| 30 | ALL | .785 | y = 1.081 x + 3.5 |
| | Lat LT 20 N | .799 | y = 1.127 x + 2.9 |
| | Lat GT 20 N | .738 | y = .922 x + 6.0 |
| 60 | ALL | .814 | y = 1.035 x + 3.8 |
| | Lat LT 20 N | .809 | y = 1.038 x + 3.1 |
| | Lat GT 20 N | .808 | y = .969 x + 6.8 |
| 90 | ALL | .803 | y = 1.011 x + 4.3 |
| | Lat LT 20 N | .825 | y = 1.031 x + 3.1 |
| | Lat GT 20 N | .684 | y = .810 x + 11.2 |

% x refers to observed wind, y refers to calculated wind
# observations south of 20 North latitude
* observations north of 20 North latitude

When all latitudes and all radii were included, the correlations of the calculated wind speeds with the observed wind speeds ranged from about 0.78 to 0.81 for both the gradient and the cyclostrophic winds. The linear regression equations are also listed in Table II. The coefficient multplying the observed wind in the linear regression equation is near 1.0 in most cases. The y intercept is generally between 2 and 5 m/s, which suggests that the observed winds are, on the average, 2 to 5 m/s lower than the calculated gradient or cyclostrophic winds. This is reasonable, because the observed winds contained random errors due to inaccuracies in the radius determination, and systematic instrument errors. Also, frictional effects were not considered. Errors are likewise introduced due to the wind averaging process. Anthes (1982) has shown that if tangential wind profiles which are in perfect gradient balance are averaged, the resultant set of averaged winds will actually be subgradient. This may provide an explanation for at least part of the discrepancy between the calculated and observed winds noted previously. The large number of correlated pairs (an average of 450 per case), together with the linear regression equations, support the contention that

the calculated winds are a good estimate of the observed winds.

Significant differences between the correlation of observed winds with gradient winds, and that of observed winds with cyclostrophic winds, were not evident. An attempt was made to discern the effects of the Coriolis parameter by evaluating the cyclostrophic and gradient winds for cyclones north and south of 20 N . Again, there was no significant difference, although the correlation coefficient was smaller for the 90 NM winds of cyclones north of 20 N. This was probably because many of the cyclones were weakening and/or undergoing extratropical transition north of 20 N. As a result, the wind and mass fields were becoming deformed to such an extent that the symmetry assumptions previously stated were no longer applicable.

The largest correlation coefficients were associated with the 60 NM winds (Fig. 1 and 2) and the lowest with the 30 NM winds (Fig. 3 and 4). It was suspected that the lower correlations at 30 NM were due to a combination of the effects of the proximity of the 30 NM observation to the eyewall, which could differ significantly from cyclone to cyclone, and the Doppler attenuation problems which can

occur in the heavy precipitation near the cyclone center. Also, since the slope of the 700 mb surface begins to change very rapidly across the region from the eyewall to the cyclone center, the centered finite difference approximation to the derivative of geopotential height with respect to radial distance may become less accurate. This is critical, since the height at the center and the height at 60 NM were used to estimate the derivative at the 30 NM radius. These computational inaccuracies could contribute to the larger amount of scatter about the linear regression "best fit" lines at wind speeds greater than 20 m/s. Since the scatter below 20 m/s is significantly less than the scatter above 20 m/s (Figs. 3 and 4), a wind speed of 20 m/s (40 kt) may indicate a threshold for accurate estimates of the inner geopotential gradient. Below 20 m/s, the finite difference approximation appears to be valid, but as the 700 mb heights fall near the cyclone center, and wind speeds increase to above 20 m/s (tropical storm intensity), the accuracy of the approximation decreases. This threshold is possibly associated with the development of the eyewall, which is a crucial stage necessary for the continued intensification of the cyclone.

It was also tested whether the error statistics at 30 NM could be improved by changing the finite differencing technique to reduce the inaccuracy in estimating the 700 mb slope across the eyewall. Therefore, the 30 NM data were also analyzed using gradient and cyclostrophic equations which evaluated the 700 mb slope at 30 NM using the height values at 30 and 60 NM, vice 0 and 60 NM. In both cases the correlation coefficients were slightly smaller (0.779 versus 0.782 for the gradient case; 0.777 versus 0.785 for the cyclostrophic case). Significant improvement was evident in the RMS errors, however (as compared to the RMS values for the centered differencing scheme listed in Table III). For the gradient case, the RMS error dropped from 11.2 m/s to 8.8 m/s. For the cyclostrophic case, the RMS error dropped from 11.69 m/s to 3.6 m/s. The decreases were probably due to the elimination of the erroneously high gradient approximations associated with the small, compact cylones. The very large reduction in the RMS error which occurred in the cyclostrophic case was probably due to the fact that the magnitude of the cyclostrophic wind is dependent entirely upon the height gradient, whereas the gradient wind magnitude is also dependent upon the Coriolis parameter. The

bias errors were of similar magnitudes, but different signs. For the gradient case, the bias changed from 4.5 m/s to -4.6 m/s. The cyclostrophic bias changed from 5.6 m/s to -3.5 m/s. This implies that the centered differencing scheme overestimated the slope and the non-centered differencing scheme underestimated it. The biggest discrepancies were evident in the comparison of the regression equations. For both the gradient and cyclostrophic cases the slope of the regression line was reduced from near 1.0 to less than 0.68. This also emphasized the overall underestimation of the height gradient by the non-centered differencing technique. Thus, no particular advantage was gained by using the non-centered differencing technique at 30 NM. Although erroneously high gradients were eliminated, erroneously low gradients were introduced. It appears that 30 NM is a critical distance where finite differencing approximations become tenuous. Some knowledge of eye radius would be necessary to choose the proper scheme for a given situation.

The primary conclusion which can be drawn from Table II is that for most purposes the mass-wind balance within 90 NM can be approximated by a cyclostrophic balance equation. An examination of the root mean square error (RMS) and the bias

values (Table III), however, indicates that a gradient balance equation may be slightly more accurate than the cyclstrophic balance equation for this data set when a centered differencing approximation to the height derivative is used. Both the 30 NM and the 60 NM RMS error and bias values are lower for the gradient equation case.

TABLE III

RMS Error and Bias Values for Gradient/Cyclostrophic Winds

| | RMS (m/s) | Bias (m/s) |
|---|---|---|
| Gradient Wind Case: | | |
| 30 NM radius | 11.20 | 4.50 |
| 60 NM radius | 7.04 | 2.40 |
| Cyclostrophic Wind Case: | | |
| 30 NM radius | 11.69 | 5.61 |
| 60 NM radius | 8.18 | 4.62 |

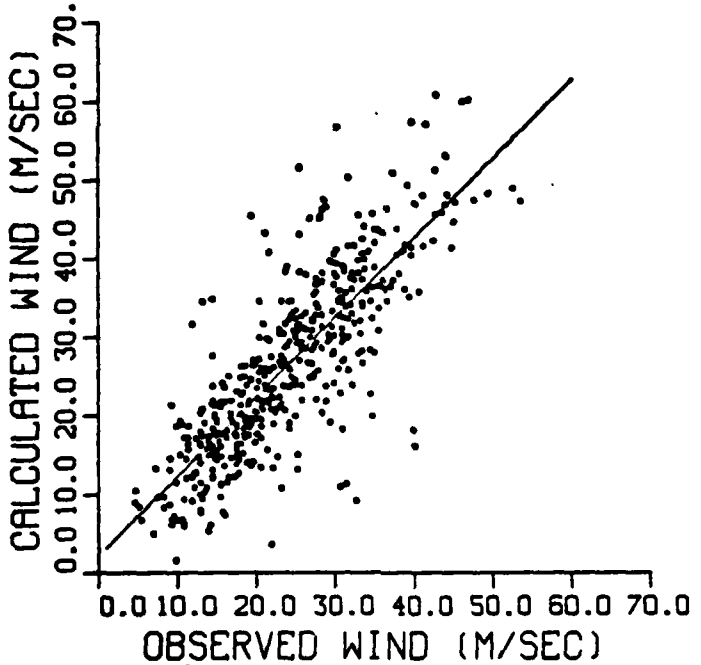


Figure 1. Calculated gradient wind (y-axis) vs observed wind (x-axis) at 60 NM radius. Winds in m/s. Curve is least squares best fit to the data.

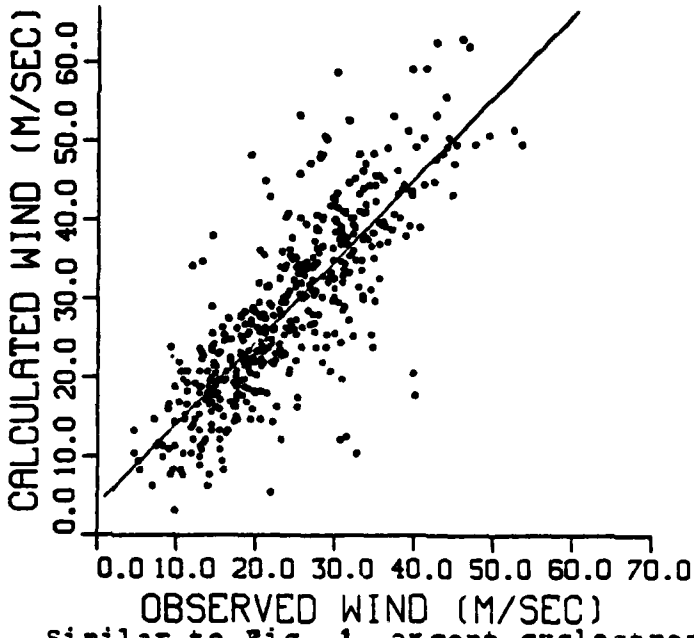


Figure 2. Similar to Fig. 1, except cyclostrophic vs observed wind.

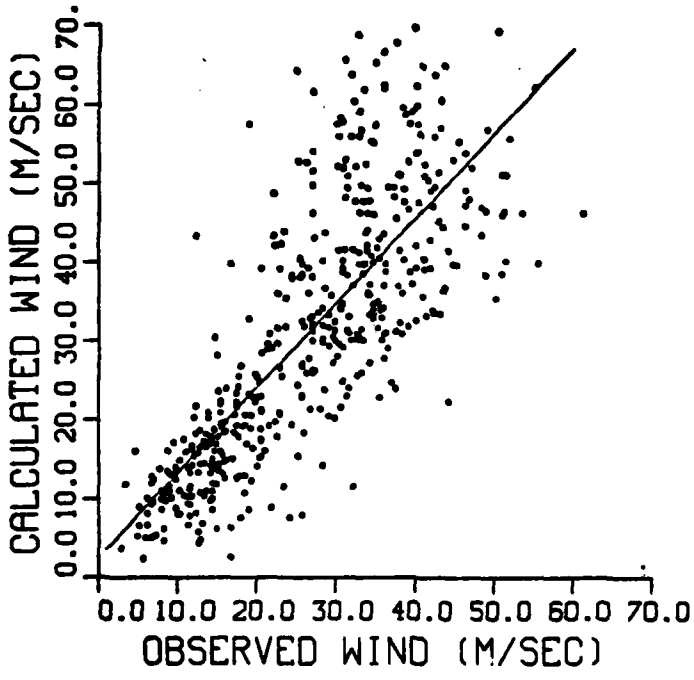


Figure 3. Similar to Fig. 1, except at 30 NM radius.

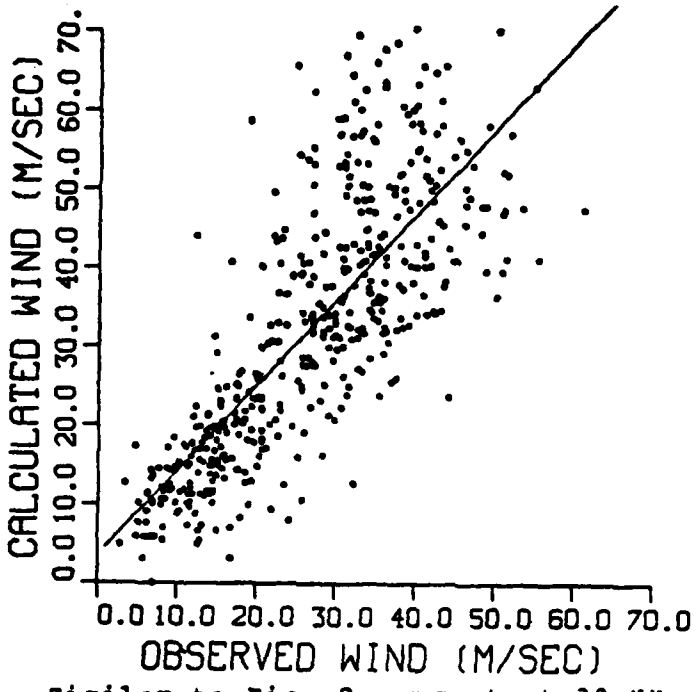


Figure 4. Similar to Fig. 2, except at 30 NM radius.

B. THE WIND SPEED-RADIUS RELATIONSHIP

It has been observed (Hughes, 1952; Malkus and Riehl, 1960; Riehl, 1963; and Shea and Gray, 1972) that the horizontal wind structure of a tropical cyclone can be represented by an equation of the form:

$$V r^x = C \qquad (5)$$

where, v = tangential wind speed

r = radial distance of observation from the cyclone center

x = constant

c = constant

Riehl (1963) assumed conservation of potential vorticity for a steady state hurricane. This assumption implies that the curl of the tangential frictional drag is equal to zero. This further implies that the partial derivative of the surface tangential stress with respect to height multiplied by the radius is equal to a constant (since the partial derivative is proportional to the frictional drag). Integrating this partial derivative from the surface to the level at which the surface stress equals zero yields the relationship: $r\tau$ = constant, where r is the radial distance from the cyclone center and $\tau$ is the surface tangential stress. If the drag coefficient is assumed to be constant, the surface tangential stress is directly proportional to the square of the tangential velocity: $\tau$ = constant $\times$ $v^2$. Combining this equation with $r\tau$ = constant produces $vr^{.5}$ = constant.

Shea and Gray (1972) calculated a value for x, in (5), of -1.05 (+/-0.6) inside the RMW (radius of maximum wind) and 0.47 (+/-0.3) outside the RMW, for profiles of flight levels between 900 to 500 mb. The latter value is very close to the value of 0.5, determined by Riehl (1963).

To calculate a value for x in (5) from the wind observations associated with the 25 tropical cyclones of this study, (5) was expressed as:

$$V r^{-x'} = C \qquad (6)$$

where, $x = - x'$

or

$$\ln V = x' \ln r + C \qquad (7)$$

For each radial leg, a least squares best fit line was determined for the set of four pairs of (ln V, ln r) points at 30, 60, 90, and 120 NM. By evaluating the slope of the (ln V,ln r) lines for many radial legs, it was possible to obtain an average x'.

The data set used for this thesis did not contain sufficient information to determine the RMW accurately. Therefore, to eliminate those situations in which the 30 NM wind observation was definitely within the RMW, only those radial legs which displayed an increase in wind speed with decreasing radius were considered. With this restriction, an average x of 0.47 (+/-0.2) was obtained for the data set. This value is exceptionally close to Shea and Gray's value, which indicates that the quality of the operational reconnaissance

data is on a par with the quality of the data collected by research aircraft.

Using the exponent value of 0.47, equation (5) was transformed to calculate the 700 mb tangential wind at radii greater than the RMW, given the wind speed at 120 NM.

$$V(r) = V(120)\left[\frac{120}{r}\right]^{.47} \qquad (8)$$

where, $V(r)$ = wind speed at radius r

$r$ = radius greater than RMW

$V(120)$ = wind speed at 120 NM

Correlations between the winds calculated using (8) and the observed winds are shown in Table IV.

TABLE IV

Correlation of Winds Calculated from Eq. (8) with Actual Winds

| Radius (NM) | Corr. Coeff. | Regression Equation (Winds in m/s) |
|---|---|---|
| "Ideal case" | 1.000 | y = 1.000 x + 0.0 |
| 30 | .735 | y = 1.071 x - 1.6 |
| 60 | .861 | y = 1.066 x - 2.9 |
| 90 | .920 | y = 1.039 x - 1.9 |

y refers to calculated wind, x refers to observed wind

For all three radii the correlation coefficients were high and the calculated regression equation was very close to the "ideal" equation. This is another demonstration that the wind observations of this data set adhere to the relationship which has been noted in previous research. This contention is further supported by the small RMS error and bias values (Table V).

TABLE V

RMS and Bias for the Wind-Radius Relationship of Eq. (8)

| Radius (NM) | RMS (m/s) | Bias (m/s) |
|---|---|---|
| 30 | 8.90 | .85 |
| 60 | 4.96 | -1.17 |
| 90 | 3.24 | -1.07 |

Figs. 5, 6 and 7 are plots of measured wind vs wind calculated from (8) for radii of 30, 60, and 90 NM, respectively. The scatter about the best fit curves decreases with increasing radius, which implies that the accuracy of the wind-radius relationship of (8) is reduced as the radius decreases from 120 NM. Specifically, the large scatter about the best fit curve at 30 NM is probably due to the proximity of the observations to the radius of maximum wind (which is not known), where the coefficient in (8) changes values. Doppler attenution problems in that region, as previously mentioned, can also produce spurious wind data.

Riehl (1963) noted that (5), with x = 0.5, appeared to hold for the tropical cyclones evaluated for his study. The tangential velocities he considered, however, were generally obtained at altitudes of several thousand feet. Therefore, it may not be proper to conclude that (5), with x = 0.5, is validated by these data. Riehl's relationship was developed from other relationships which involved surface tangential stress, but these 700 mb observations are somewhat above the surface frictional layer. Also, the assumption that the drag coefficient is constant throughout the tropical cyclone may be questioned. It may be more correct to refer to (5), with x = 0.47, as simply an empirically derived equation, without attempting to give a physical interpretation to the relationship between wind and radius.

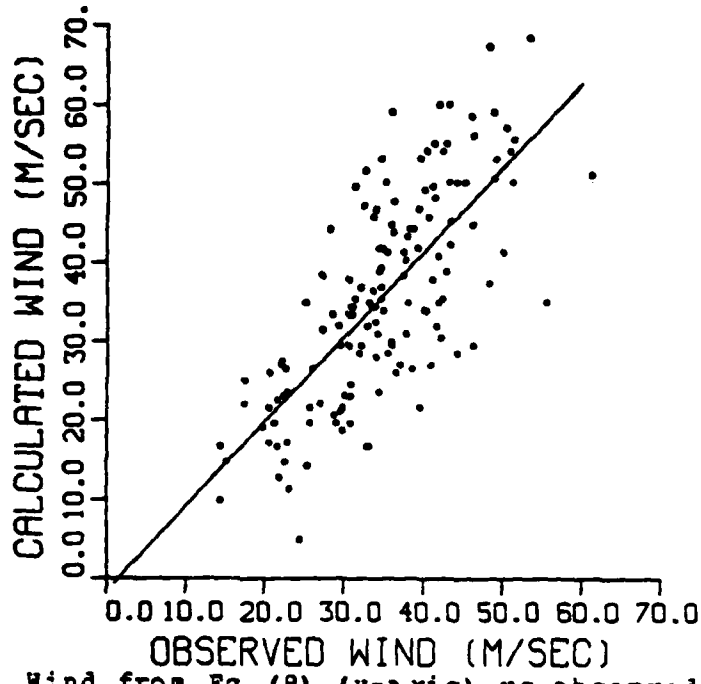


Figure 5. Wind from Eq. (8) (y-axis) vs observed wind (x-axis) at 30 NM. Curve is least squares best fit to data.

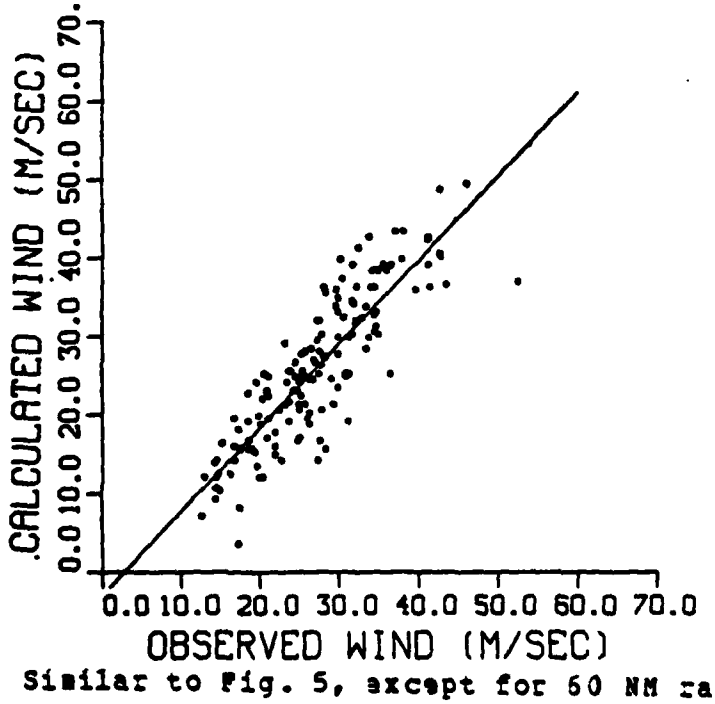


Figure 6. Similar to Fig. 5, except for 60 NM radius.

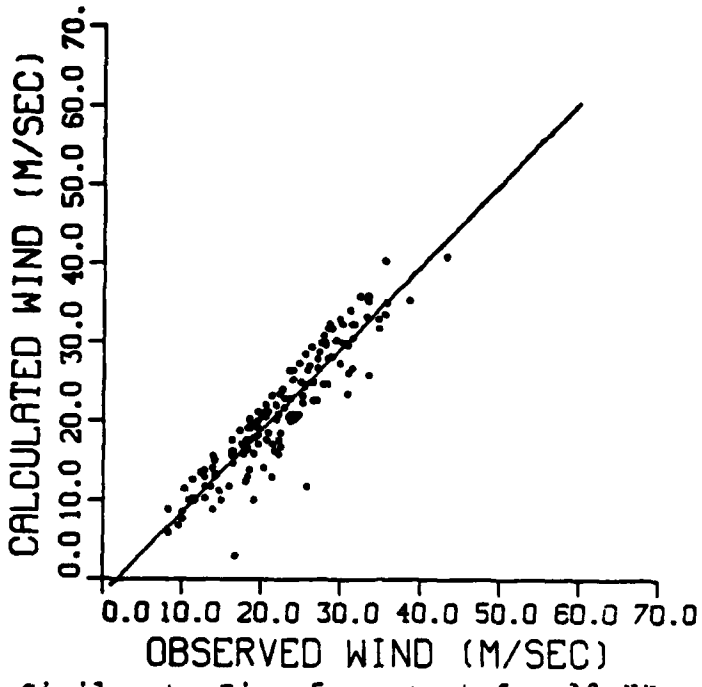


Figure 7. Similar to Fig. 5, execpt for 90 NM radius.

# IV. THE MOIST STATIC ENERGY/INTENSIFICATION STUDY

## A. REVIEW OF TROPICAL CYCLONE INTENSIFICATION THEORIES

For the purposes of this study, tropical cyclone intensity and change in intensity were arbitrarily defined in terms of central surface pressure. Sheets (1969) showed that the 100 mb surface in the vicinity of a hurricane is not altered by the presence of the tropical cyclone. Thus, the central surface pressure is directly proportional to the mean temperature of the column of air over the center (by the hypsometric equation). An analysis of the relationship between central surface pressure (as determined by extrapolation from 700 mb) and 700 mb center temperature (a crude estimate of the mean temperature of the air column), produced a correlation coefficient of -0.68 for the data of this study. Given the large number of temperature/pressure pairs evaluated (476), a coefficient of this size implies that the two parameters are related, as was expected (Fig. 8).

The temperature/pressure relationship described above is a cornerstone of most tropical cyclone development theories.

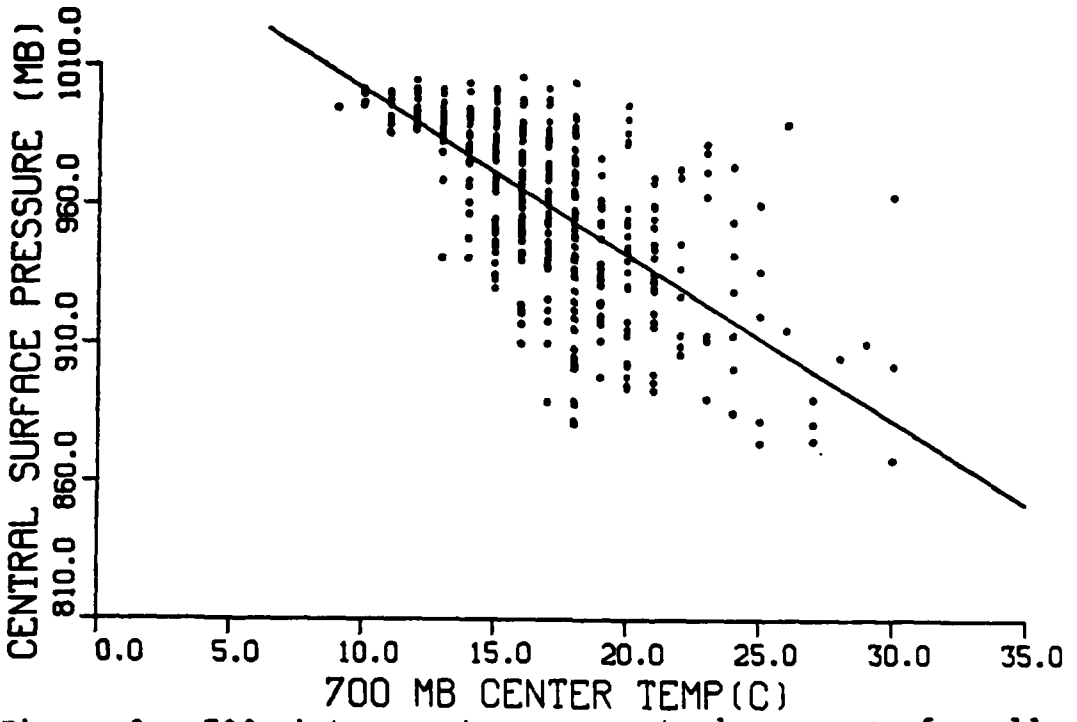


Figure 8. 700 mb temperature vs central pressure for all cyclones. Curve is least squares best fit to data.

A prevailing theory of tropical cyclone intensification (e.g. Anthes, 1982) involves a rather complex series of feedback mechanisms dealing with the release of latent heat and the associated vertical adjustments, which are not yet fully understood. A simplified explanation of this theory is as follows. As low-level air spirals toward the center of a developing tropical cyclone, the temperature and moisture content are increased due to fluxes of heat and water vapor from the sea surface and downward transfer of heat from above due to entrainment mixing and subsidence. When

this low-level air reaches the eyewall it begins to rise rapidly. Cooling due to expansion eventually induces condensation and the resultant release of tremendous amounts of latent heat. Rather than increasing the ambient temperature within the eyewall, the latent heat instead is transformed into potential energy by increasing the buoyancy of the air. Once the air reaches the top of the eyewall some of it is eventually entrained into the eye where it is forced to subside. The physical process responsible for this subsidence is one of the phenomena which is not fully understood. The subsiding air within the eye warms by compression and produces a decrease in the surface pressure. Thus, the sensible and latent heat which the air acquired as it passed over the ocean surface eventually is manifest as an ambient temperature increase and, therefore, pressure drop, within the eye. The drop in surface pressure increases the inflow near the surface which in turn enables the inflowing air to absorb still larger amounts of sensible and latent heat energy and the vertical circulation is enhanced. Some of this energy continues to find its way into the eye where it causes still further temperature increases and associated pressure drops, and the feedback cycle continues. The

tangential wind near the center increases, as the vertical circulation intensifies, due to conservation of angular momentum. Once a tropical cyclone is deprived of its source of latent and sensible heat, as is the case when it moves over land, for example, dramatic weakening can occur.

As emphasized by Holland (1983), clouds are a crucial factor in the intensification process. Besides providing the latent heat which controls the strength of the vertical circulation, the clouds also provide for a local recycling of mass. This recycling produces warming necessary to maintain a balance between the mass field and the developing wind field under the vertical circulation. Also, Gray (1979b) suggests that the recycling induces a local enhancement of the evaporation from the sea surface which helps balance the export of moist static energy by the vertical circulation (Holland, 1983).

The simplified description of tropical cyclone development presented above, known as the CISK (conditional instability of the second kind) theory, was proposed by Charney and Eliassen (1964). Other research (as summarized by Holland, 1983, for example) has indicated that the CISK theory does not adequately explain all aspects of tropical

cyclone development. Ramage (1959) hypothesized that positive vorticity advection downstream of an upper-level trough in the westerlies could induce upper-level divergence over an incipient tropical cyclone. The low-level convergence associated with the upper-level divergence could then lead to intensification. Riehl (1975) has proposed that a tropical cyclone may intensify if a nearby cold upper-level tropospheric low collapses. A secondary circulation is set up by the subsiding air in the cold low and the rising air in the cyclone. Intensification occurs as angular momentum is transported inward at low levels. Sadler (1978) has noted the relationship between tropical cyclone development and the position of the Tropical Upper-Tropospheric Trough (TUTT) relative to the cyclone. He suggests that the establishment of easterly and westerly outflow channels by the TUTT increases the ventilation of heat away from the cyclone. This process appears to result in intensification, although a complete explanation of how upper-level outflow patterns affect intensity change is lacking. In addition to the intensification mechanisms described above, which rely to a great exent on thermodynamic processes, a purely dynamic intensification mechanism has also been proposed.

Conservation of angular momentum produces regions of negative vorticity at upper levels near the center of a tropical cyclone. The outflow air can become inertially unstable if this negative vorticity exceeds the planetary vorticity. In this situation, outward acceleration at upper levels would develop. Mass continuity would require surface convergence, pressure falls and, therefore, cyclone intensification. Although inertial instability is evident in tropical cyclone models, it has not been directly observed (Black and Anthes, 1971, for example).

From the discussion above, it seems probable that tropical cyclone intensification is controlled by the interaction between the cyclone and the synoptic scales of motion, as well as the interaction between the moist convection and the cyclone scales of motion (CISK), as suggested by Holland (1983). The role of the synoptic scale environment may be to assist in organizing the moist convection fields to permit optimum exploitation by the cyclone scale environment. Although tropical cyclone intensification is controlled by the dynamic interaction between the cyclone and synoptic scale environment, it is ultimately dependent upon the moist convection (Holland, 1983).

Clearly, there is a direct relationship between the strength of the vertical circulation and the intensity of the tropical cyclone. The more vigorous the vertical circulation, the lower the central surface pressure and the greater the tangential wind speed near the central region. Since the vertical circulation is controlled to a great extent by the clouds near the circulation center, it is plausible to assume that a relationship may exist between changes in the near-center cloud energetics and subsequent changes in cyclone intensification. It would not be necessary to know the exact cause of the change in cloud energetics (which may involve complex interactions) in order to evaluate the effects of such changes.

## B. AN EQUIVALENT POTENTIAL TEMPERATURE STUDY

One parameter that can be used to estimate the energy of a parcel of air (the non-kinetic portion) is the equivalent potential temperature, since it takes into account the energy due to both sensible and latent heat. Malkus and Riehl (1960) attempted to determine the relationship between a change in equivalent potential temperature and a corresponding change in surface pressure. They began with the assumption that the conditions within the eyewall of a

tropical cyclone are very nearly moist adiabatic. This was later verified by Riehl (1970). The hydrostatic equation was then integrated to determine the surface pressure under the eyewall assuming that the 100 mb level was undisturbed. Because the air was assumed to be saturated, the equivalent potential temperature within the column was constant with height and the temperature at any level could be determined from a moist adiabat. Using this technique, and solving for different values of equivalent potential temperature, Malkus and Riehl (1960) developed the following relationship:

$$\Delta P = -2.5\left(\Delta \theta_e\right) \tag{9}$$

where, $\Delta P$ = surface pressure change under eyewall

$\Delta\theta_e$ = equivalent potential temperature change

Using aircraft reconnaissance data for Atlantic tropical cyclones and a linear regression method, Riehl (1963) determined the following empirical relationship:

$$\left(P - 1005\right) = -2.56\left(\theta_e - 350\right) \tag{10}$$

where, $P$ = surface pressure under eyewall

$\theta_e$ = equivalvent potential temperature

(1005 and 350 are reference values)

Bell and Tsui (1973) found similar results from a set of northwest Pacific tropical cyclones, except the coefficient was determined to be -2.25 vice -2.56.

The results of the above studies give a strong indication that a change in equivalent potential temperature is a necessary, though probably not sufficient, condition for tropical cyclone intensification. It is further implied that those processes which govern the transfer of sensible and latent heat to the lower atmosphere ( sea surface temperature and wind speed, for example) also have a significant influence on the intensification pattern of a tropical cyclone.

Tropical cyclones typically deepen at rates of less than 1 mb/hour, but occasionally a cyclone will undergo a period of rapid, or even explosive, deepening. Holliday and Thompson (1979) defined rapid deepening as a pressure drop of 30 mb in 24 hours (-1.25 mb/hour) and explosive deepening as a drop of 30 mb in 12 hours (-2.5 mb/hour). The majority of tropical cyclones in the northwest Pacific which reach super-typhoon strength (maximum sustained surface wind speeds of at least 130 kt, or a minimum central surface pressure less than about 911 mb) attain that intensity

following a period of explosive intensification (Holliday and Thompson, 1979).

Two attempts have been made to develop techniques which could be used to forecast explosive deepening based on 700 mb equivalent potential temperature. Sikora (1976) analyzed dropsonde and upper air sounding data associated with tropical cyclones in the northwest Pacific. An evaluation of the available data indicated that the potential for explosive deepening increased when the 700 mb equivalent potential temperature exceeded 370$^{o}$K. Sikora was quick to point out, however, that his results were based on a small data set and therefore may not be conclusive. Dunnavan (1981) developed an intensity forecasting technique for northwest Pacific tropical cyclones which involves monitoring the relationship between the minimum sea level pressure at the cyclone center and the central 700 mb equivalent potential temperature as determined by aircraft. Simultaneous pressure and temperature values are plotted verses time on the same graph. The vertical pressure and temperature axes are oriented, based on an empirically derived relationship, so that explosive deepening is anticipated if the pressure and temperature traces intersect. This technique has shown some skill and is currently used operationally by forecasters at the JTWC.

## C. A PROPOSED INTENSITY CHANGE RELATIONSHIP

There is significant evidence to support the contention that at least some of the change in tropical cyclone intensity can be directly related to changes in equivalent potential temperature. If this is indeed the case, it can be assumed that a steady, constant increase in equivalent potential temperature would be associated with a steady, constant decrease in central surface pressure, and therefore, an increase in intensity. Likewise, a sudden increase in the equivalent potential temperature of the air moving into the eyewall might be expected to produce a subsequent sudden decrease in surface pressure, and thereby initiate a period of explosive deepening. Rapid or explosive deepening may often be due to the arrival, at the base of the eyewall, of a "pulse" of air of significantly higher equivalent potential temperature. These pulses could be the result of an increase in the strength of the northeast trade winds, a surge in the southwest monsoonal flow or areas of anomalously high sea surface temperatures, for example. In each case the low-level moisture content, and therefore equivalent potential temperature, could be increased significantly.

If such pulses do exist, it may be possible to detect their presence from the reconnaissance aircraft data before they reach the base of the eyewall. The detection of a pulse before it reaches the eyewall might provide a forecaster with advance notice that conditions favorable for a rapid change in intensity were developing. Significant lead time may be possible because a period of time is required for the latent and sensible heat in the low-level air to be transported from the ocean surface to the interior of the eye, where it can produce the surface pressure drop.

## D. ASSUMPTIONS NECESSARY TO EVALUATE INTENSITY CHANGE

By compositing rawinsonde data for many Atlantic tropical cyclones, Gray (1979a) was able to show that the strongest inflow exists below 800 mb within 120 NM of the tropical cyclone center (Fig. 9). Thus, the high equivalent potential temperature air flows toward the eyewall in a region which is generally below the flight level (700 mb) flown by the reconnaissance aircraft in the northwest Pacific.

Frank (1977) has determined that the maximum vertical motion associated with a tropical cyclone also occurs within 120 NM of the cyclone center. Since at least some of the near-surface air is advected upward through the 700 mb

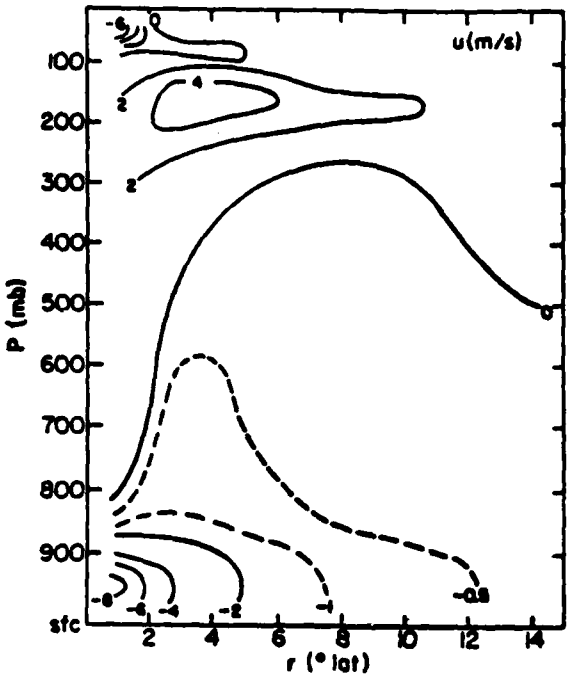


Figure 9. Composite cross section of the radial wind component (m/s), azimuthally averaged, for western Atlantic Ocean tropical cyclones (Gray, 1979a).

level, it is assumed that any fluctuations in the near-surface equivalent potential temperature would be reflected at the 700 mb level where it could be detected by a reconnaissance aircraft. A detailed analysis of Hurricane Inez by Hawkins and Imbembo (1976) showed that substantial variation existed in the horizontal equivalent potential temperature field. Vertical variations, however, appeared to follow a pattern (Fig. 10). Areas of lower (or higher) equivalent potential temperature at 700 mb appeared to extend vertically into the regions below 700 mb, as indicated by

the vertical orientation of the contours. Based on the Hurricane Inez study, the assumption is made that the equivalent potential temperature at 700 mb is related to the equivalent potential temperature in the radial inflow layer below.

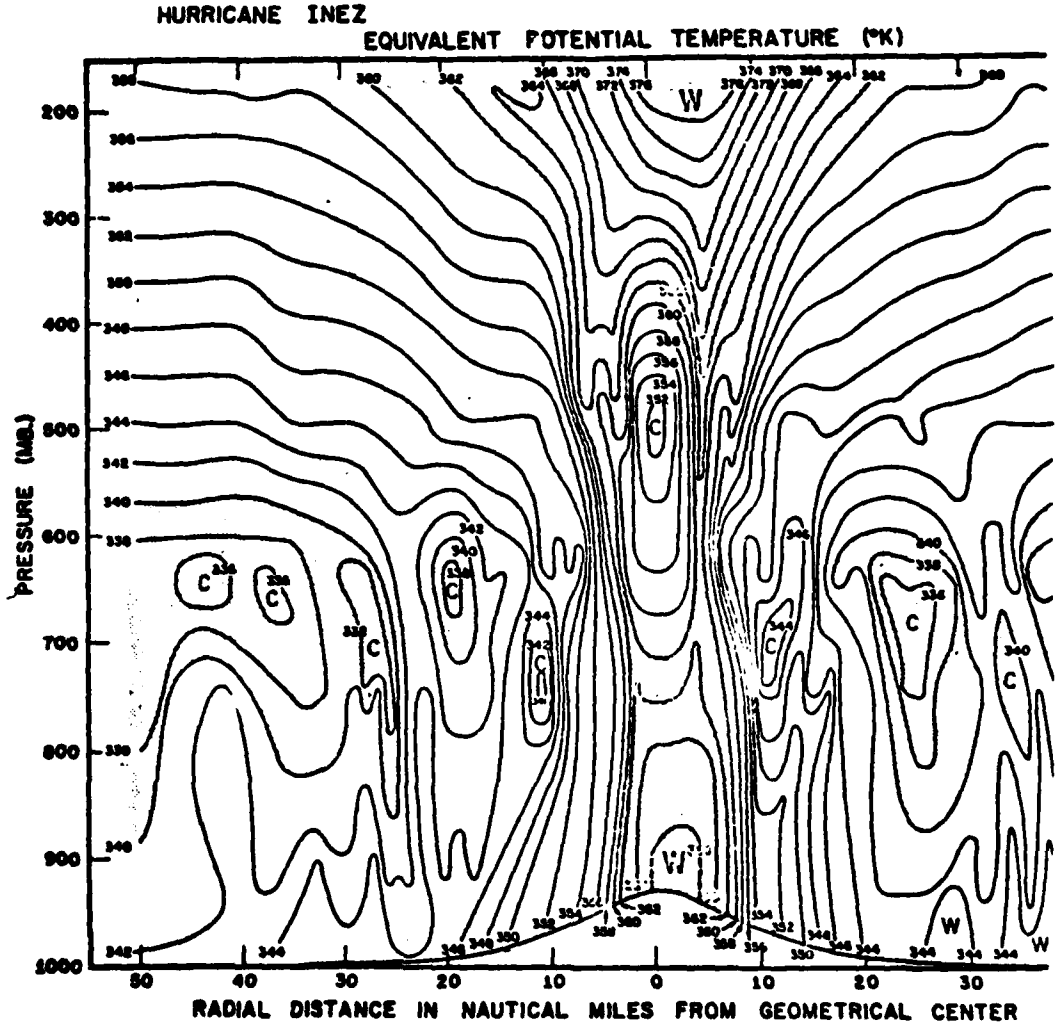


Figure 10. Vertical cross section of equivalent potential temperature (K) for Hurricane Inez on 28 September, 1966 (Hawkins and Imbembo, 1976).

Another assumption must be made concerning the averaging of the data for the 25 tropical cyclones of this study. Ideally, the tropical cyclones would exhibit axi-symmetry with respect to the temperature and dew point fields (and, therefore, the equivalent potential temperature field) in the horizontal. If this were the case, then it would be possible to assume that an average of the inbound and outbound flight leg temperature and dew point values, at a given radius, would be representative of the entire cyclone for that radius. Clearly, complete symmetry is not often observed (e. g. the field in Fig. 10 for Hurricane Inez, 1966).

It is assumed that the change in central pressure will be due to the net change in equivalent potential temperature of the low-level air which is arriving at the eyewall from all directions. Thus, if high equivalent potential temperature air from one semicircle of the cyclone arrives at the eyewall at the same time that low equivalent potential temperature air arrives from the opposite semicircle, they may tend to offset, so that no significant change in the intensification trend would occur. An average of the equivalent potential temperatures for the two semicircles in the

above example would likely result in an equivalent potential temperature which would be consistent with a steady development trend. However, if high equivalent potential temperature air arrives from both semicircles, the average of the two potential temperatures would be large and significant intensification would be anticipated.

Because the aircraft reconnaissance data of this study were used to analyze the equivalent potential temperature/intensity change relationship, it was necessary to assume that the data obtained for a radial leg were representative of the semicircle that they were centered on. This is probably a good assumption for developing cyclones (which are the main focus of this study). The assumption begins to break down, however, as the cyclones begin to fill and become extratropical.

Equivalent potential temperature values are extremely sensitive to the amount of water vapor present in the air. Therefore, to minimize the effects of extreme fluctuations in moisture associated with random encounters with rainbands, the emphasis of the study is on the 30 NM observations. It was hoped that the relative humidity would be more consistent in that area since clouds and precipitation tend to concentrate more uniformly near the cyclone center.

Moist static energy is a measure of the "total effective energy", since it takes into account both the sensible and latent heat contained in an air parcel (Hawkins and Rubsam, 1968). The equation which defines moist static energy can take the form:

$$H = C_p T + gz + Lq \qquad (11)$$

where,

H = moist static energy per unit mass

Cp = specific heat of dry air at constant pressure

T = air temperature

g = acceleration of gravity

z = height of pressure surface

L = latent heat of condensation

q = mixing ratio of parcel

It can be shown (Holton, 1979) that moist static energy is approximately conserved when equivalent potential temperature is conserved. Therefore, moist static energy was calculated rather than equivalent potential temperature, since H is more easily evaluated.

## E. EVALUATION OF THE INTENSITY CHANGE RELATIONSHIP

Fourteen of the 25 tropical cyclones of this study had data records of sufficient length and detail to describe their evolution. Four of these 14 cyclones attained surface central pressures of 911 mb or below following a period of rapid intensification. The average pressure drop was approximately -1.7 mb/h ( -80.0 mb/48.0 h ), which lies between the rapid and explosive deepening rates defined in Chapter IV. Graphs of central surface pressure versus time and averaged 700 mb moist static energy (at 30 NM) versus time were prepared for each tropical cyclone. The four rapidly deepening cyclones were evaluated because their rapid intensification periods were similar. The remaining 10 cyclones could not be compared because their intensification and moist static energy trends had very little in common. However, the graphs of two of these: typhoon Owen and super typhoon Judy are contrasted with the four rapid deepening cyclones in subsection 2.

### 1. Four Rapidly Deepening Tropical Cyclones

An examination of the graphs of the four rapidly deepening tropical cyclones (Figs. 11-14) indicates that the moist static energy reached a peak at or just prior to the

period of rapid deepening, and decreased during the subsequent 48 hours. The noteable exception is super typhoon Irma (Fig. 14) whose 30 NM moist static energy continued to increase during the 48-h deepening phase. Irma may have been an atypical cyclone, however, since her 700 mb eye temperature never exceeded 20 C. This is very low compared to the typical values of 26 C or higher which have been observed for tropical cyclones of her intensity (JTWC, 1980 and 1982, for example).

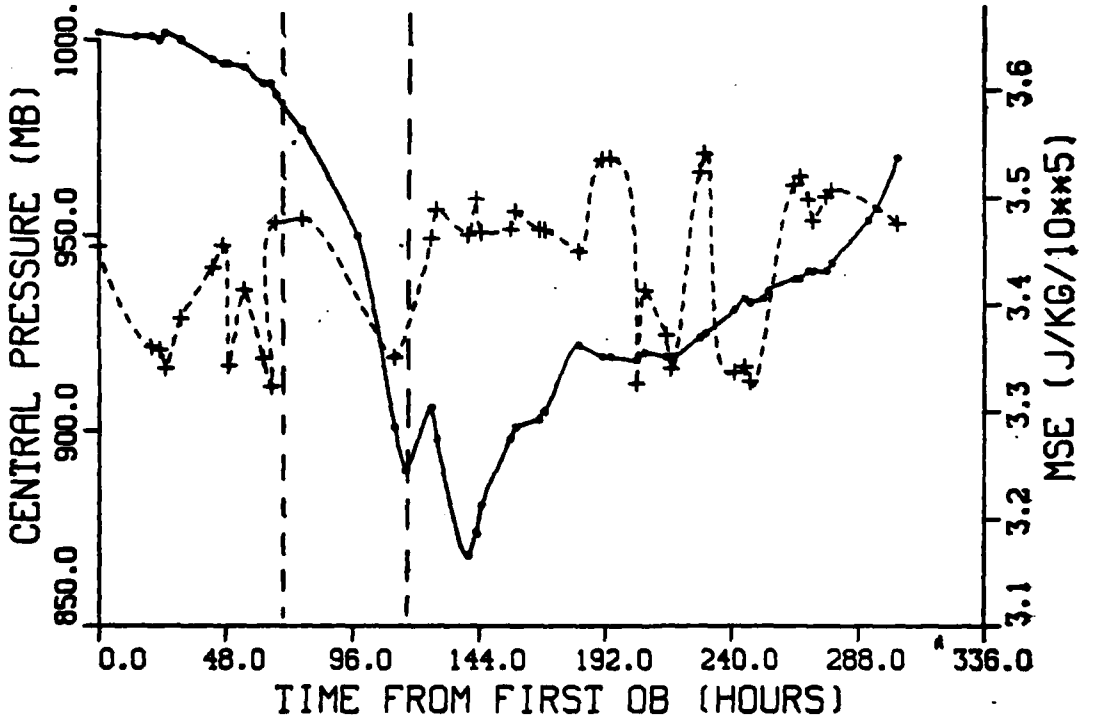


Figure 11. Pressure and moist static energy vs time curves for ST Tip. Solid curve is surface pressure and dashed curve is 700 mb moist static energy at 30 NM. Vertical dashed lines indicate 48-h period of most rapid deepening.

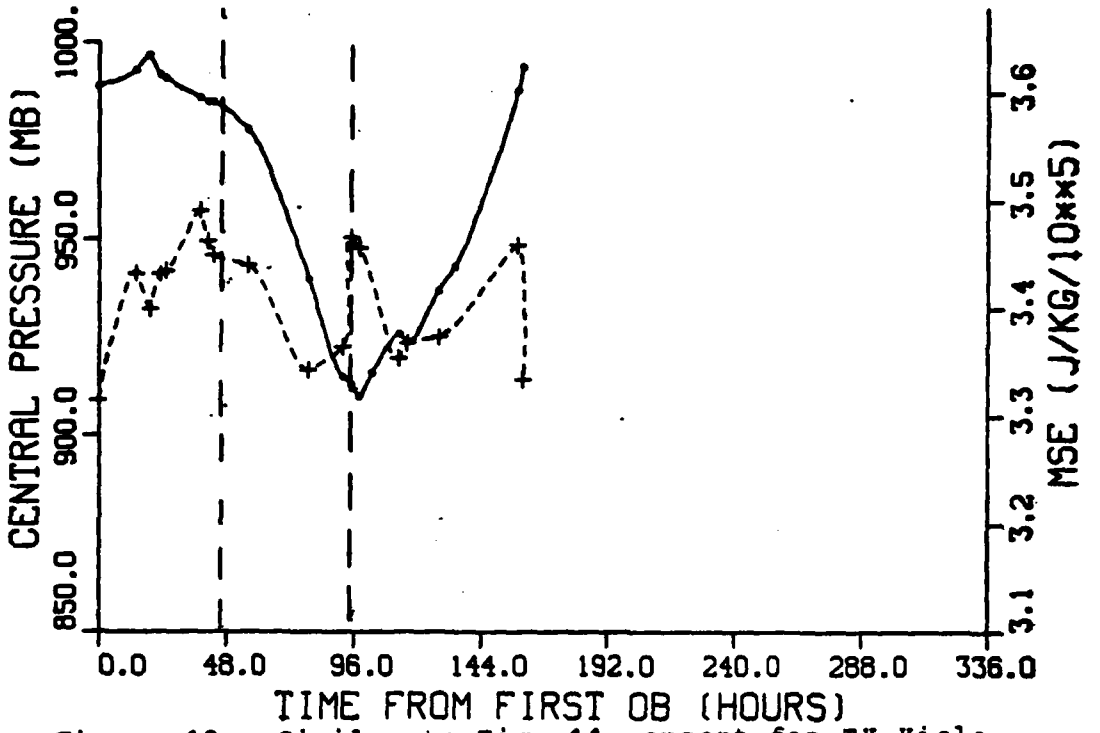


Figure 12. Similar to Fig. 11, except for TY Viola

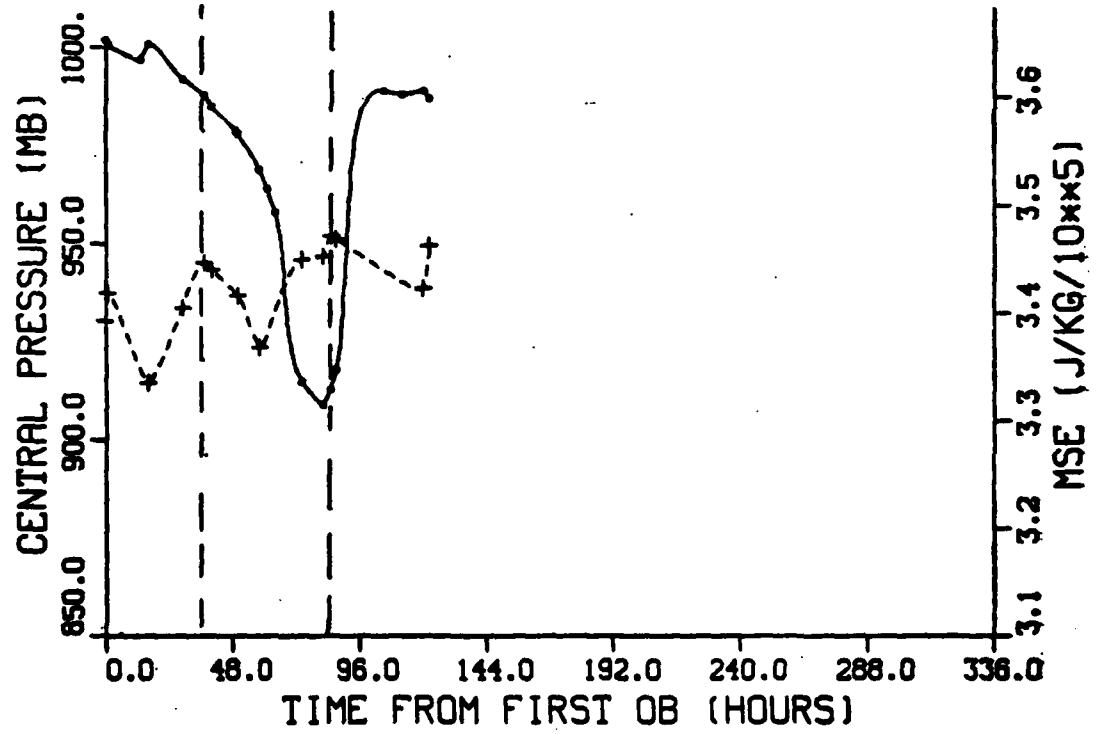


Figure 13. Similar to Fig. 11, except for ST Kim

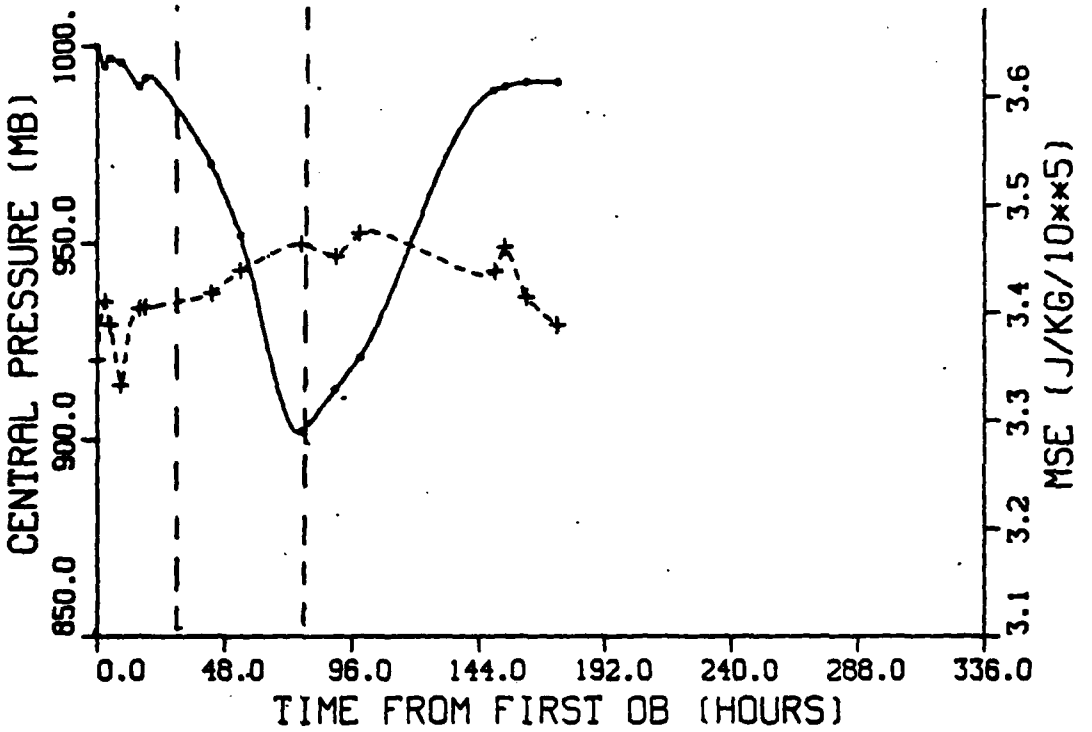


Figure 14. Similar to Fig. 11, except for ST Irma

The pressure and moist static energy correlations indicated in Figs. 11-14 are consistent with the moist static energy/intensity change relationship discussed in Chapter IV. The peaks in moist static energy prior to the rapid deepening phase may indicate the arrival, at the 30 NM point, of pulses of high equivalant potential temperature air. The response to these pulses (i. e. rapid surface pressure drop) occurs during the subsequent 48 h. The decrease in moist static energy during the 48 h intensification period implies that air with lower equivalent potential

temperature had replaced the high potential temperature air at 30 NM, outside the eyewall. The response to the lower equivalent potential temperature air (i.e. a pressure rise) is not manifest until after the rapid intensification period ends. A sharp pressure rise after the minimum central surface pressure was reached, was observed in all four cases. It should be noticed that super typhoon Tip (Fig. 11) ultimately continued to deepen (to a record 870 mb) after the initial rapid deepening phase. Immediately after the 48-h deepening period, however, aircraft reconnaissance revealed a short-lived period of pressure increase (Fig. 11) which may correspond to the previous decrease in moist static energy.

The moist static energy/intensity change relationship presented in Section C suggests that a sudden increase in equivalent potential temperature is associated with a subsequent decrease in central surface pressure. This implies that the magnitude of the moist static energy change, and the period over which it occurs, may be of greater importance than the magnitude of the peak value. The moist static energy curves of three of the four rapidly deepening tropical cyclones indicated a rapid increase (to a

peak) prior to the 48-h deepening period. It can be speculated that the decrease in the moist static energy of super typhoon Tip prior to the final rise (Fig. 11) may be due to smaller scale fluctuations, which were encountered by the aircraft at 30 NM by chance. Also, it should be noted that the fourth rapidly deepening typhoon, Irma (Fig. 14), did not display a sharp jump in moist static energy prior to rapid intensification, but instead followed a steady increasing trend.

2. Examples Contrary to the Relationship

Two other tropical cyclones, typhoon Owen (Fig. 15) and super typhoon Judy (Fig. 16), also experienced abrupt increases in moist static energy, but these increases occurred during, rather than prior to, the deepening phase. The peak moist static energy values were attained about 24 h prior to the time of minimum central pressure. Unlike the four rapidly deepening cyclones above, these two did not develop to maximum intensity during a single rapid deepening period, but instead, intensified in spurts. This made it more difficult to evaluate the relationship of moist static energy change and pressure change. Also, the significant pressure decreases prior to the rapid increase in moist

static energy, can not be explained solely by the moist static energy/intensity relationship proposed in Section C.

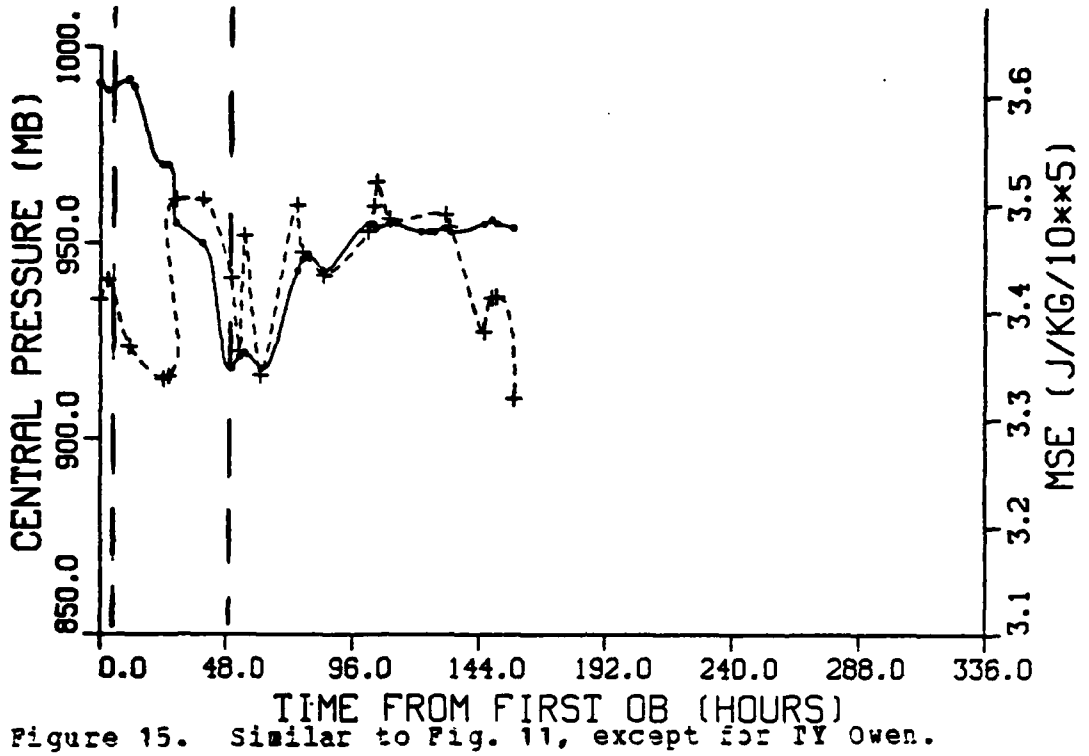


Figure 15. Similar to Fig. 11, except for TY Owen.

Peak values, or periods of rapid increase of moist static energy were not confined to the tropical cyclone developing phase only, as is indicated by Figs. 11-16. In fact, the highest values and most extreme fluctuations often occurred during the filling stage (Figs. 11 and 16, for example). This may be due to the expansion of the inner-core region (as the tropical cyclone weakens) which could place the 30 NM observations in the high equivalent

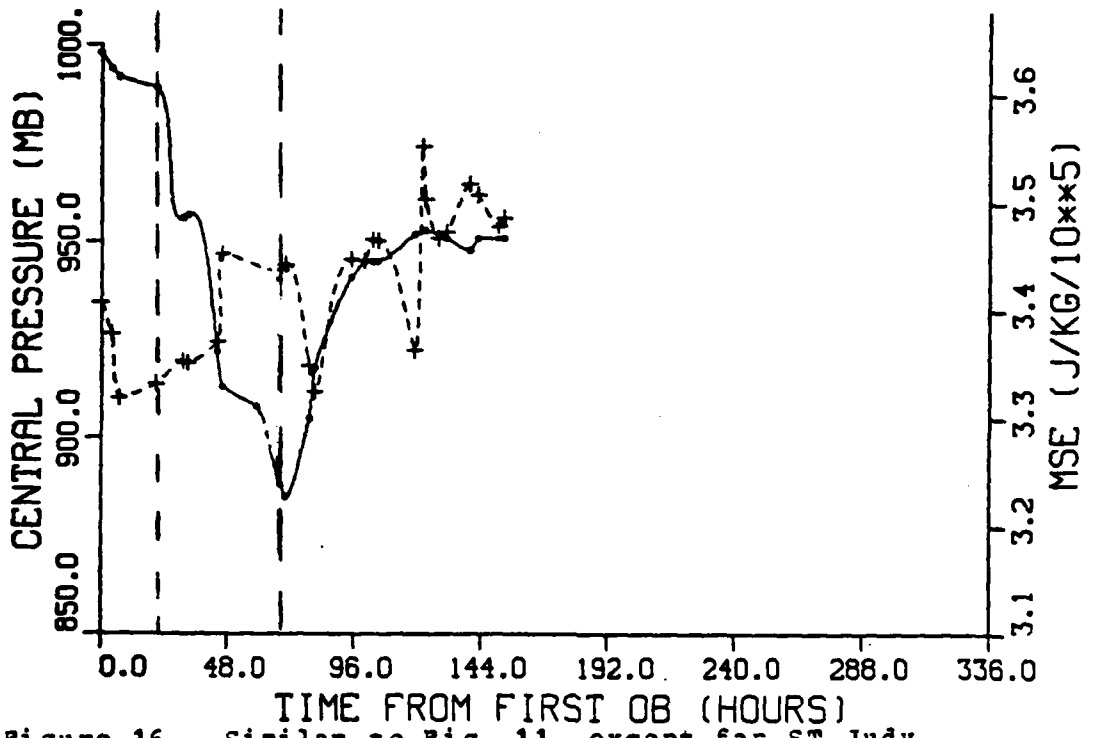

Figure 16. Similar to Fig. 11, except for ST Judy.

potential temperature air within the eye. Also, a general breakdown in the tropical cyclone structure due to extra-tropical transition could cause the averaging assumption to become questionable, especially if the cyclone developes large asymmetries in the horizontal temperature and height fields. Large differences between successive moist static energy observations (which are especially noticable during the weakening stages) probably arise because each observation provided the thermodynamic properties for only one section of the cyclone. Any one observation may define thermodynamic values which are radically different from the

values obtained for other sections of the cyclone which were observed on previous or subsequent aircraft reconnaissance missions. In this situation, no one temperature or dew point observation can be thought of as representative of the cyclone as a whole. As previously stated, it was hoped that this problem could be reduced by considering moist static energy changes at 30 NM, but Figs. 11-15 indicate that this procedure was not entirely successful. Another way to minimize this problem would be to examine the moist static energy changes in specific quadrants. This technique was not used for the northwest Pacific data of this study, however, because the time period between successive observations in any particular quadrant was too long to permit a meaningful evaluation of the rapid intensity change relationship.

3. Re-examination of the Intensity Change Relationship

Given the central pressure and moist static energy fluctuations above, it is virtually impossible to correlate a specific moist static energy change with the subsequent pressure change. This problem may be compounded by the variability in the time period between observations and the differences in the intensification trends of the individual

cyclones. Typhoon Alice (Fig. 17) and super typhoon Rita (Fig. 18) illustrate this problem. A good correlation may exist, but the time and space resolution of the northwest Pacific aircraft reconnaissance data may not be high enough to permit an evaluation of the cause and effect relationship. It is, however, possible to compare the four rapidly deepening tropical cyclones, because they have something in common: a 48-h period when they were deepening at a similar rate. It is assumed that the processes responsible for the deepening were the same for each cyclone.

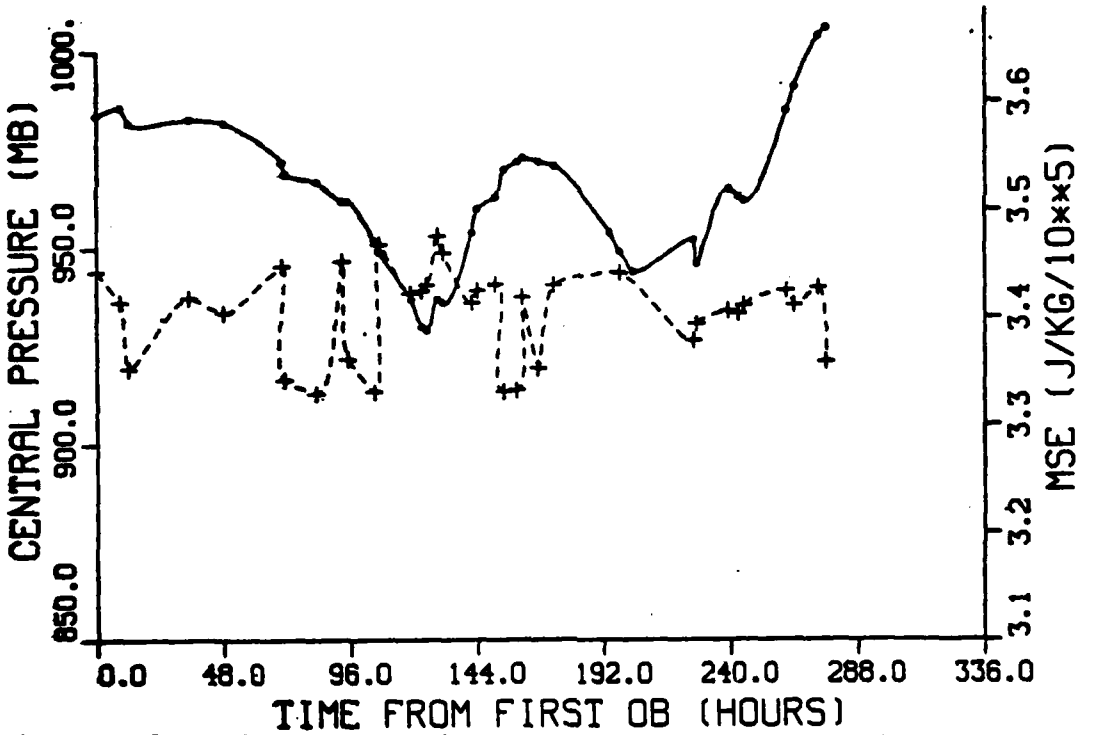


Figure 17. Similar to Fig. 11, except for TY Alice.

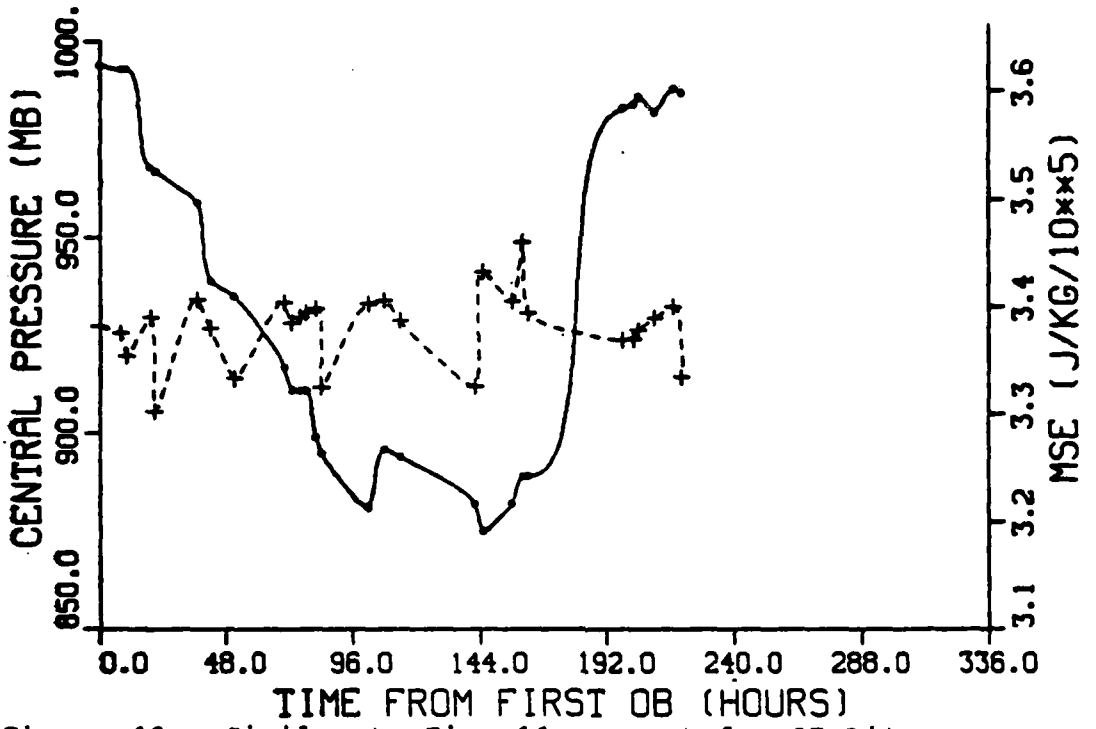

Figure 18. Similar to Fig. 11, except for ST Rita.

During the tropical cyclone developing state, the assumption of horizontal symmetry in the low-level temperature and height fields is probably reasonable. However, horizontal moisture fluctuations appear to be substantial. Fluctuations in moist static energy are due almost entirely to the latent heat term in (11), as illustrated by the curves of H and dry static energy (CpT + gz) for super typhoon Tip (Fig. 19). Since the difference between the curves is the latent heat term (Lq), it is apparent that the fluctuations in H must be due primarily to the moisture content of the air. Therefore, the quality of a moist static

energy estimate is dependent upon how representative the dew point observations are at a particular radius.

A representative moisture value for a particular radius is the most difficult parameter to determine from the aircraft data. It had been hoped that non-representative dew point observations could be minimized by examining moist static energy close to the center (30 NM). However, the dew point values are highly dependent upon the location of the aircraft relative to the convective elements near the center. The rapid fluctuations evident in the moist static energy curve for super typhoon Tip's moist static energy curve (Fig. 19) during the filling stage are also probably due to this effect.

The areal extent of a pulse of high equivalent potential temperature air may also be as important as the magnitude of the moist static energy. A narrow pulse of high energy air may have little effect on changing the intensification trend of the entire tropical cyclone. To determine whether a sudden increase in moist static energy at 30 NM was associated with a pulse of significant horizontal extent, curves of moist static energy versus time for radii from 0 to 120 NM were constructed. If peaks in the

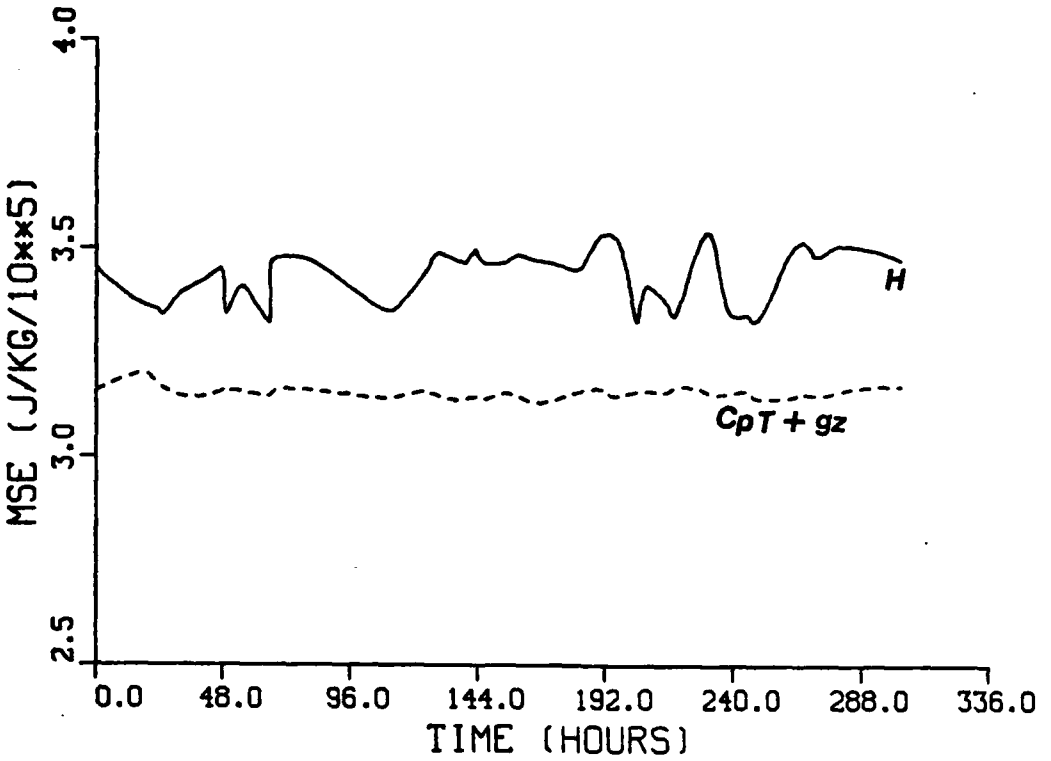


Figure 19. Moist static energy (H) and dry static energy (CpT+gz) versus time for ST Tip.

moist static energy curves at 30 NM coincided with peaks at 60 NM or 90 NM, it would give an indication of the width of the approaching pulse. The increase in the moist static energy of typhoon Viola (Fig. 20) at 30 NM, prior to the period of most rapid deepening, is reflected at 60 NM, and possibly at 90 NM. In the case of super typhoon Tip (Fig. 21), however, it is questionable whether the smaller peaks at 60 and 90 NM are actually a reflection of the peak at 30 NM. The peak in the 30 NM moist static energy of super typhoon Kim (Fig. 22) prior to rapid deepening appears to be

reflected out to 120 NM. However, the amplitude of the peak becomes quite small at the larger radii. Although typhoon Irma did not reach a definite peak prior to rapid deepening, her rapid deepening is probably keyed to the steady increase in moist static energy at 30 NM during that period. But this steady increase is only weakly (if at all) reflected in the curves for greater radii (Fig. 23). Typhoon Alice (Fig. 24) is an example of a tropical cyclone which did not undergo a significant period of rapid deepening. The moist static energy curves do not correlate well with the exception of a brief period when she had reached maximum intensity (centered near 144 h). The implication of Figs. 20-24 is that a pulse of high equivalent potential air which is large enough to induce a period of rapid deepening must not only be evident at 30 NM, but must be reflected at the 60 NM or greater radii as well.

There is a problem which arises, however, when aircraft data from cyclones of different sizes are analyzed. For example, super typhoon Tip (Fig. 21) and super typhoon Rita (Fig. 25) attained similar minimum central surface pressures (876 mb for Rita; 870 mb for Tip), but they differed significantly in size. Rita was an extremely compact

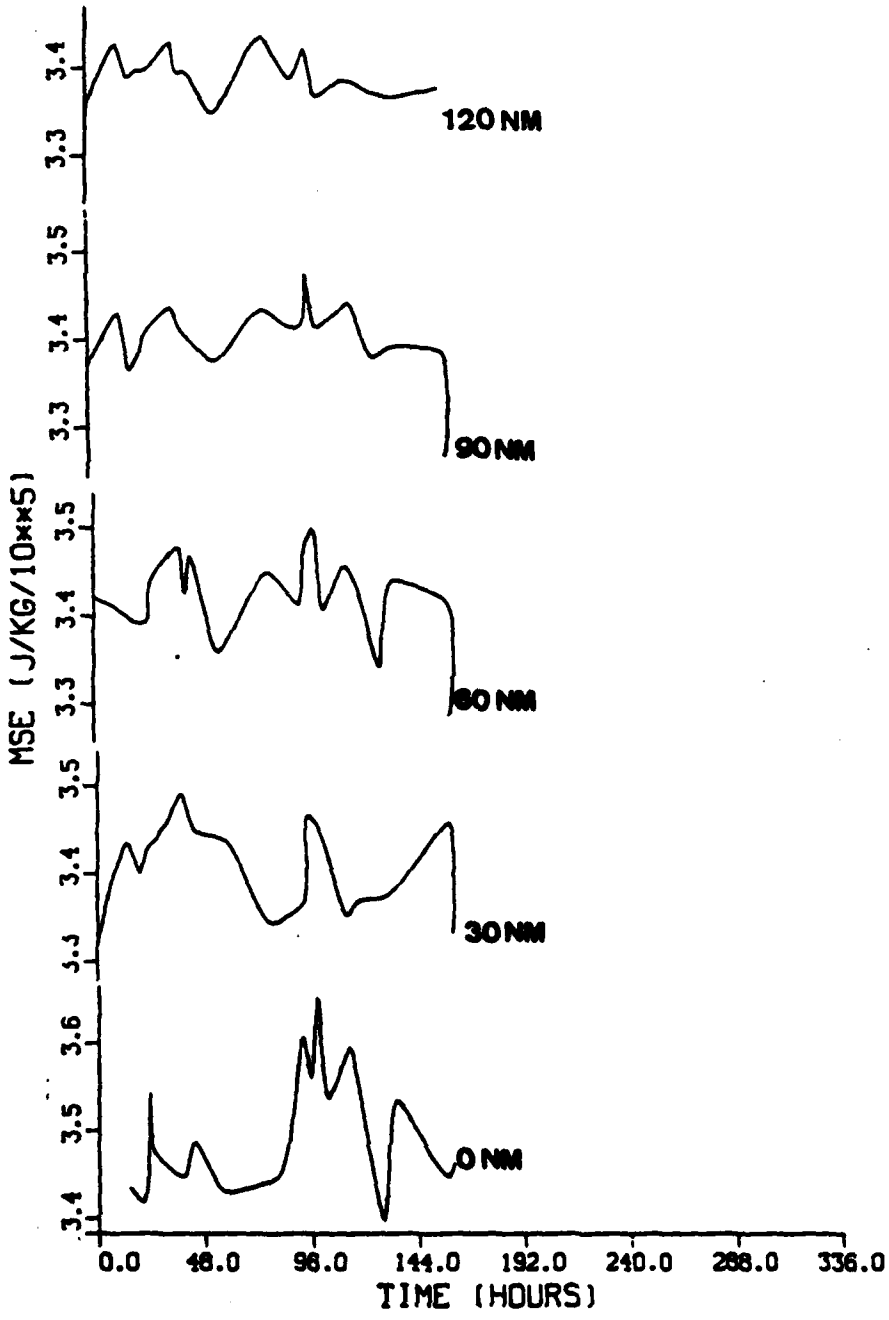


Figure 20. Moist static energy versus time for typhoon Viola at radii from 0 to 120 NM.

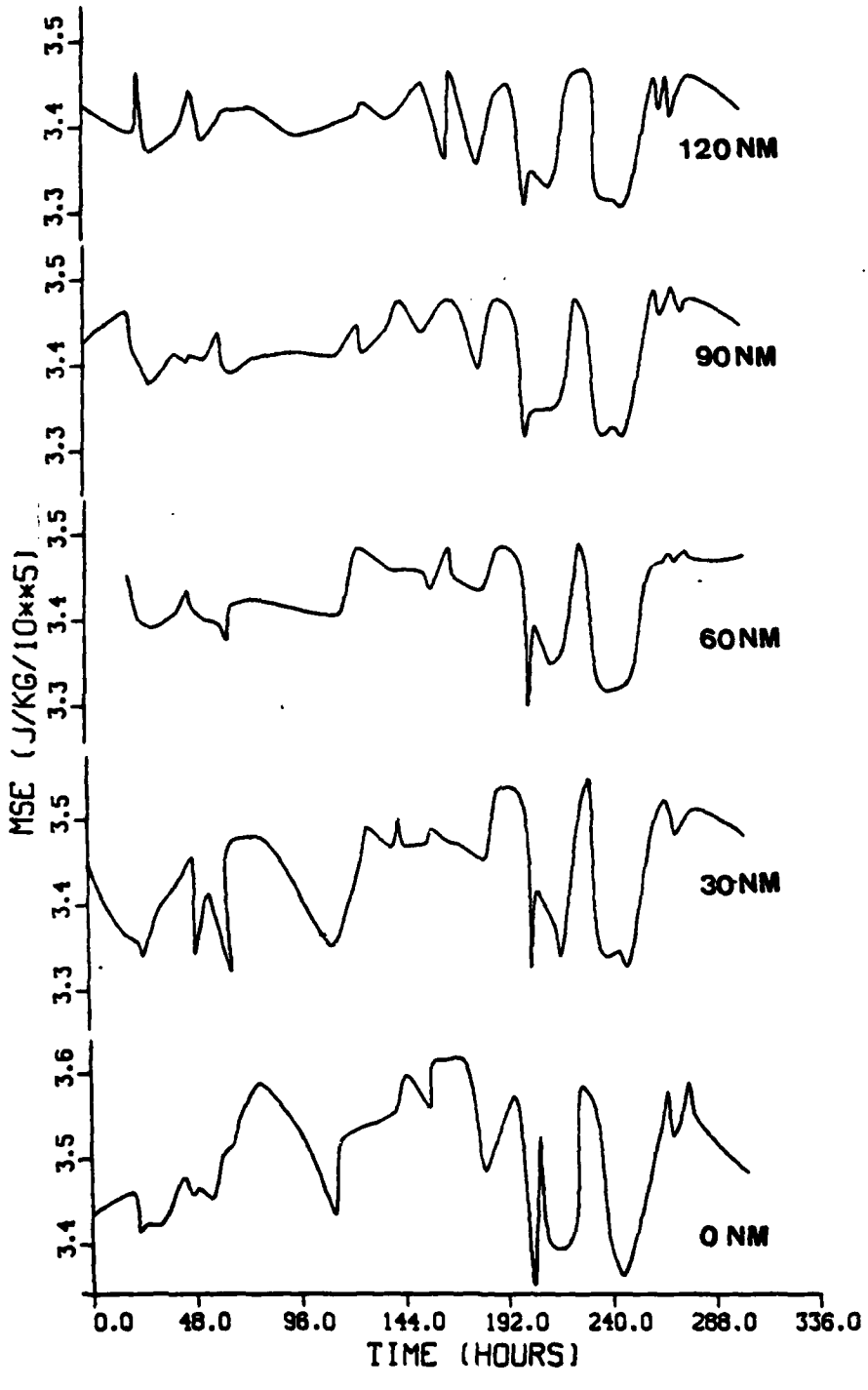


Figure 21. Similar to Fig. 20, except for super typhoon Tip.

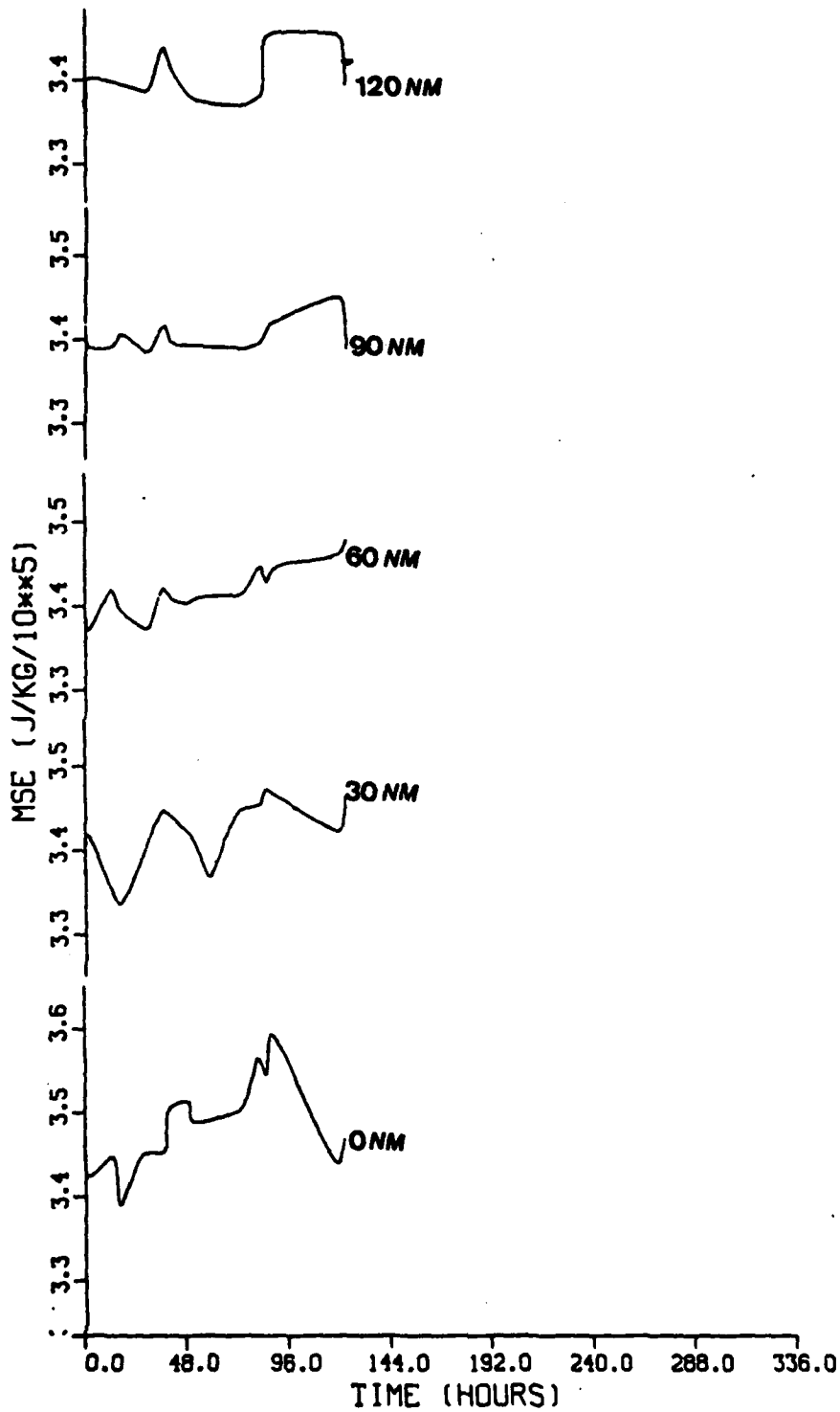


Figure 22. Similar to Fig. 20, except for super typhoon Kim.

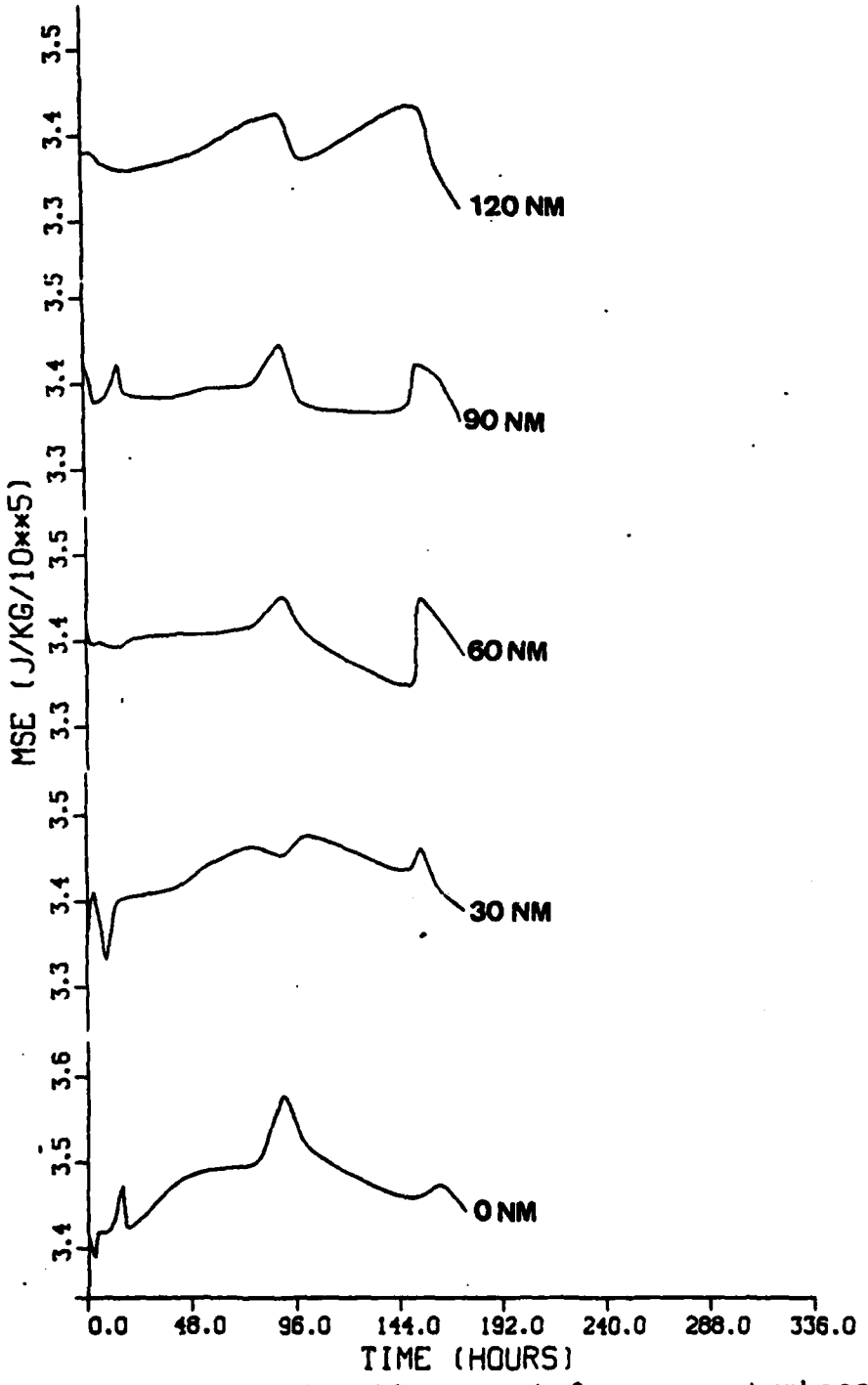


Figure 23. Similar to Fig. 20, except for super typhoon Irma.

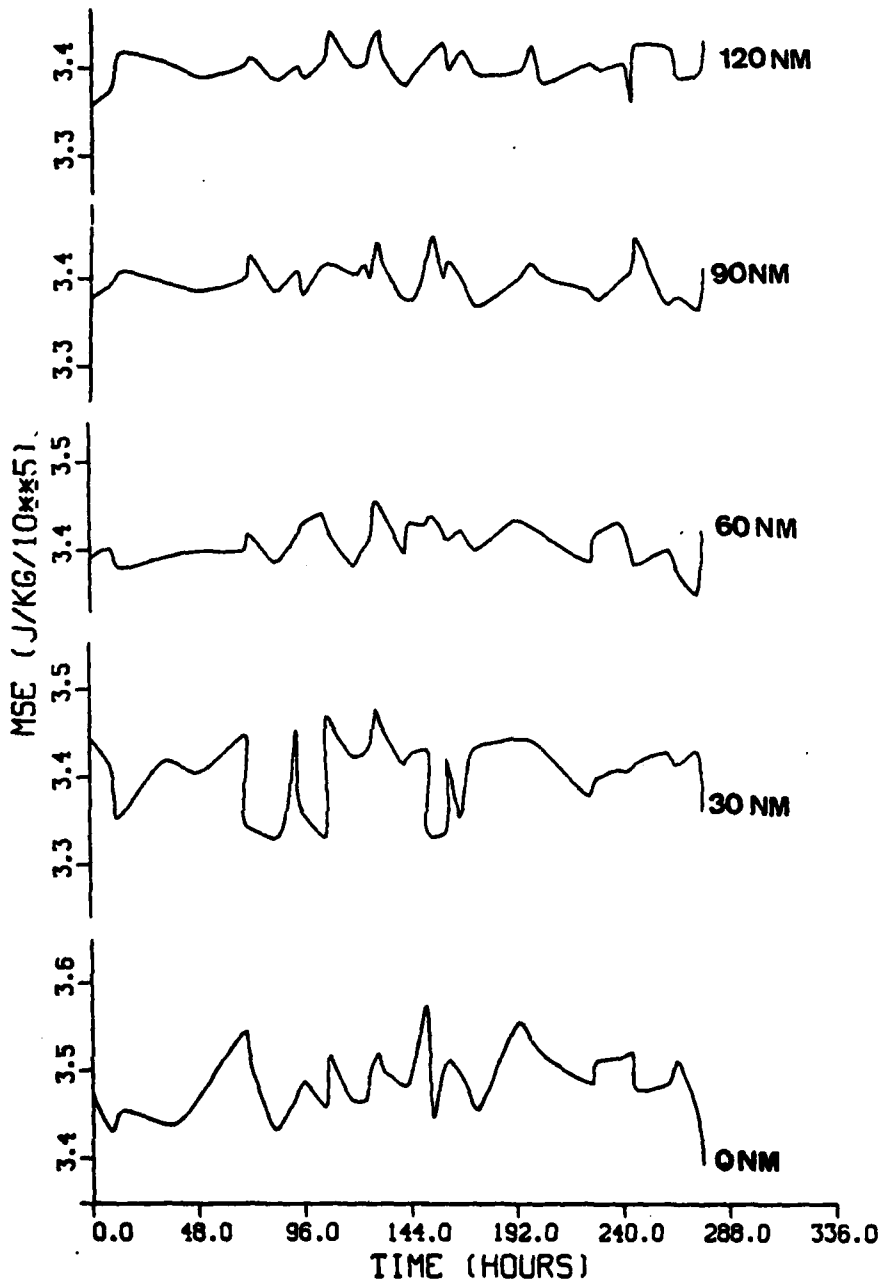


Figure 24. Similar to Fig. 20, except for typhoon Alice.

system, with a 30 kt wind radius of less than 185 NM. On the other hand, Tip was the largest tropical cyclone ever observed, with a 30 kt wind radius of 600 NM (Dunnavan and Diercks, 1980). This size difference is manifest in their moist static energy curves. Fluctuations in Rita's moist static energy curve at 30 NM are only weakly (if at all) reflected at radii greater than 30 NM. The fluctuations in Tip's moist static energy at 30 NM, however, are strongly reflected at greater radii. This is most noticeable from the 96 h point until dissipation.

The size difference is further illustrated by correlations of the 30 NM moist static energy value with the values at 60, 90 and 120 NM for Tip (Fig. 26) and Rita (Fig. 27). The correlation coefficients for Tip are generally higher than those for Rita. This is especially noticeable when the 30/60 NM correlation curves for the developing phase (curves labelled c) are compared. For both cyclones, the best overall correlations are for the weakening phases (curves labelled a). The very high coefficients for Tip (0.92 or greater) illustrate the strong influence of the central region, which extends out to at least 120 NM. In contrast, the corresponding smaller coefficients for Rita

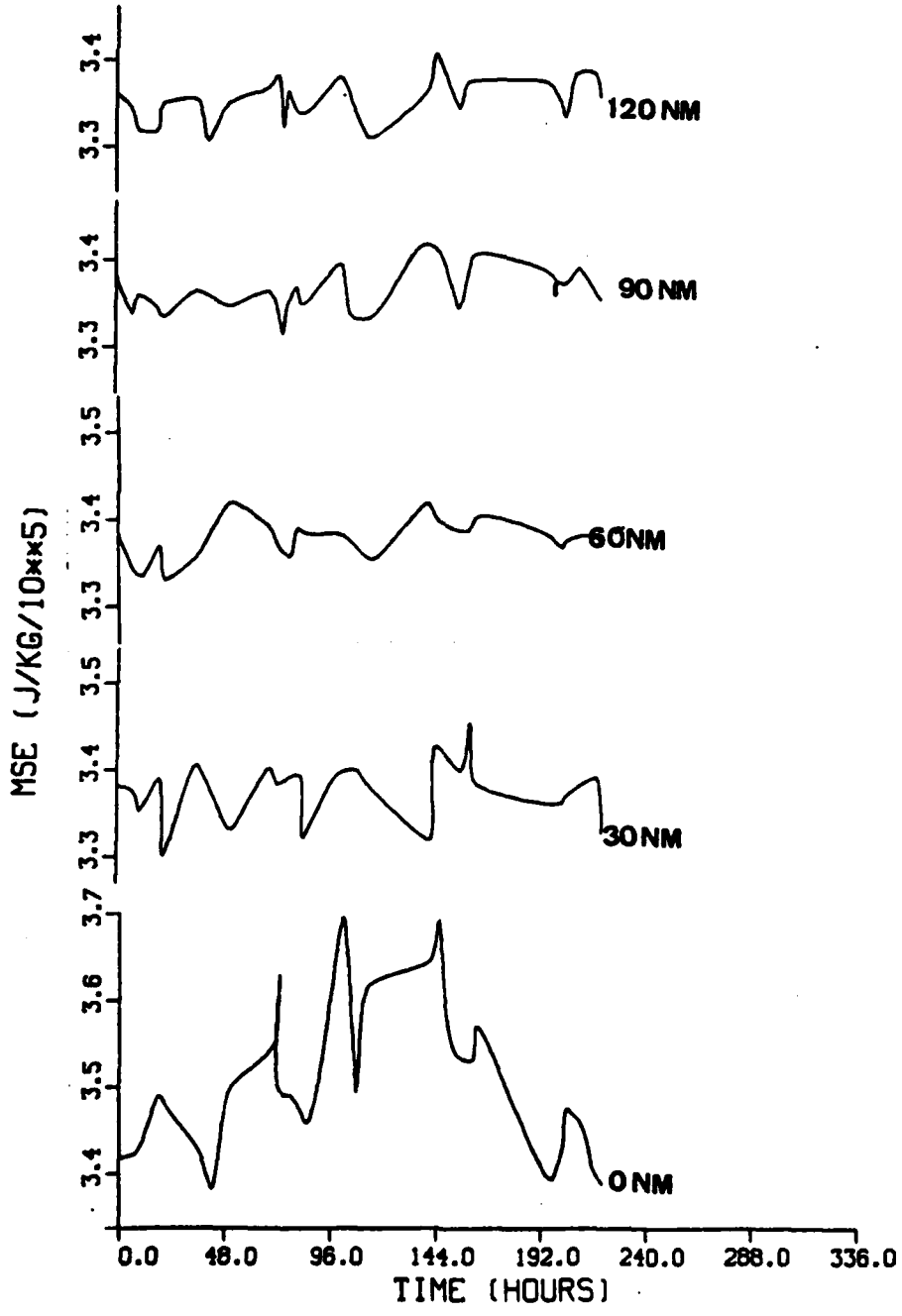


Figure 25. Similar to Fig. 20, except for super typhoon Rita.

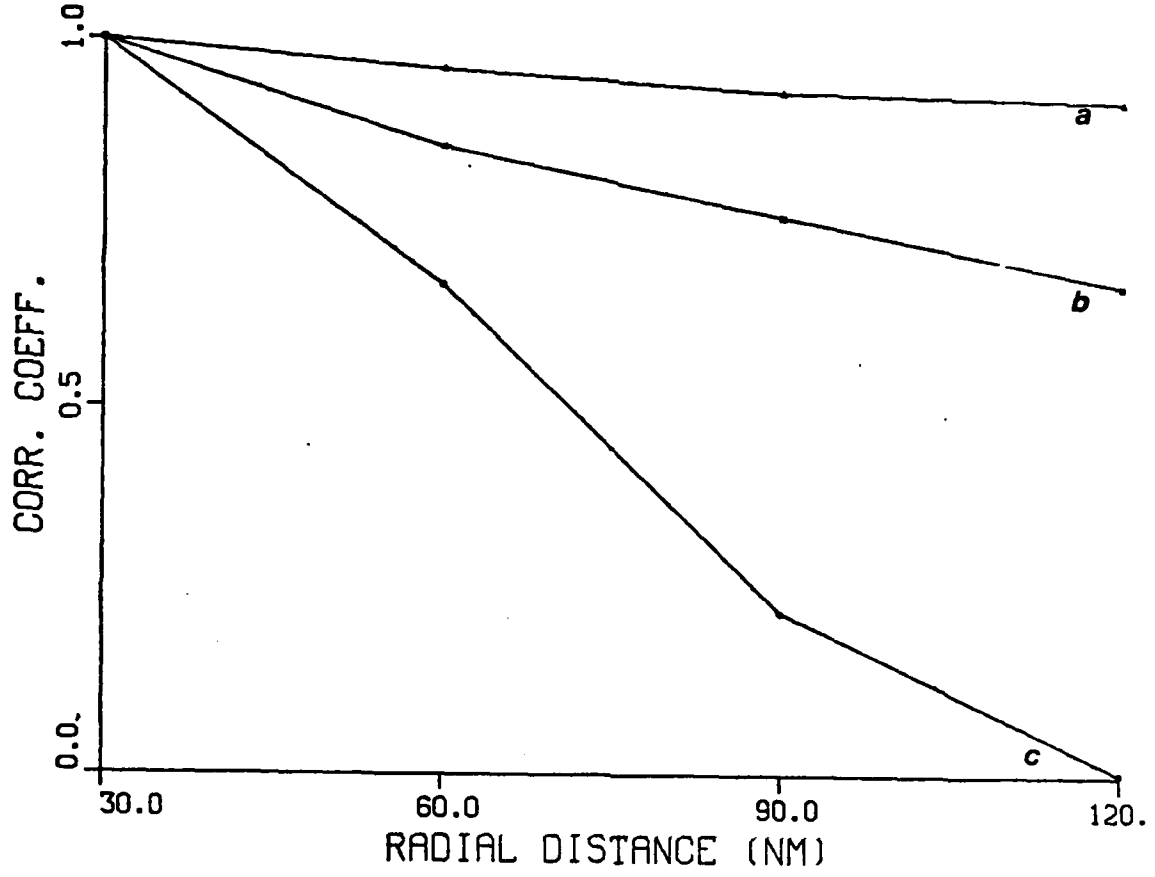


Figure 26. Correlation of ST Tip's 30 NM moist static energy with corresponding moist static energy values at 30, 60, 90 and 120 NM. Curve (a) is correlation of observations obtained after maximum intensity was reached; curve (b) is correlation of all observations; curve (c) is correlation of observations obtained prior to the time of maximum intensity.

(0.60 to 0.46) indicate that the influence of the center region decreases rapidly with distance from the center.

These two cases illustrate a significant problem which can not be resolved with the available aircraft reconnaissance data. It is impossible to determine the dimensions of a high potential temperature pulse if the data are

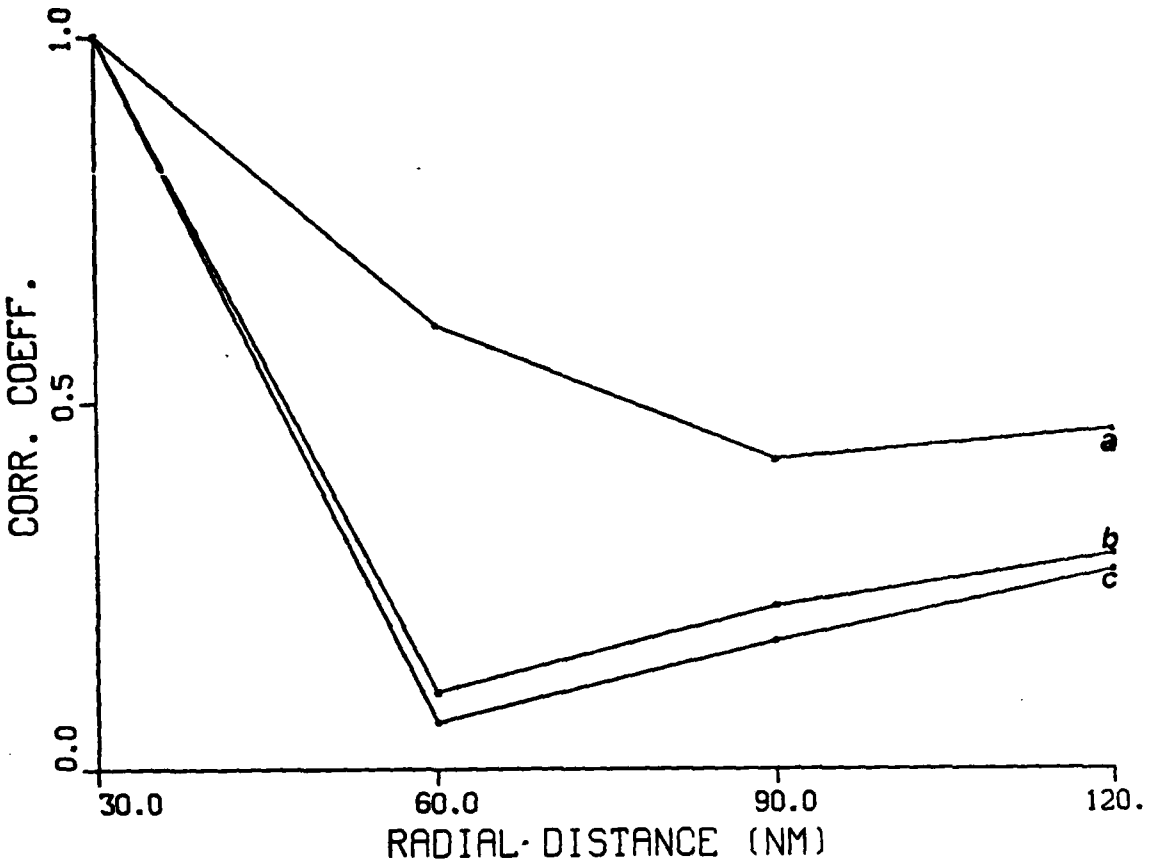


Figure 27. Similar to Fig. 26, except for ST Rita.

always restricted to observation points at 30 NM intervals from the 120 NM point to the center, without regard to the variability in size of the cyclones. In the case of extremely large tropical cyclones (e.g. Tip), the influence of the cyclone's center may extend to beyond 120 NM, making it difficult to determine the size of a pulse which is moving into the cyclone from the environment. Likewise, 30 NM resolution may be too coarse to permit the detection of

subtle changes in the moist static energy in the vicinity of an extremely compact cyclone (e.g. Rita).

4. Summary

Clearly, a change in the equivalent potential temperature is not the only mechanism which is related to tropical cyclone development. Upper-level divergence and changes in angular momentum, for example, may also be important. Periods of rapid deepening which might be expected to occur due to changes in equivalent potential temperature may not develop because of an unfavorable upper-level divergence pattern. It was not possible to determine when the fluctuations of moist static energy at a particular radius reflected a genuine increase. The non-representativeness of the moist static energy values could be reduced, but not eliminated, by analyzing 30 NM data. It is thus concluded that it is not possible to fully evaluate the moist static energy/intensity change relationship using the limited northwest Pacific tropical cyclone data.

## V. CONCLUSIONS

An analysis of the reconnaissance aircraft data of 25 northwest Pacific tropical cyclones produced results which are consistent with empirical relationships obtained by earlier researchers with Atlantic tropical cyclones. The mass-wind fields of the cyclones determined from these aircraft data were found to satisfy a cyclostrophic balance relationship. However, an examination of RMS and bias errors of observed winds versus winds calculated from the mass field revealed that a gradient balance realtionship was slightly more accurate, as was anticipated (Holton, 1979).

The aircraft reconnaissance data were also used to evaluate a long established wind-radius relationship:

$$V r^x = C$$

Shea and Gray (1972) obtained a value for x, using Atlantic tropical cyclone data, of 0.47(+/-0.3) for radii outside the radius of maximum wind (RMW). For the 25 northwest Pacific tropical cyclones of this study, an x value of 0.47 (+/-0.2) was calculated. Riehl (1963) also justified a value of x of 0.5 by assuming a surface tangential stress-wind speed

relationship and that the curl of the tangential frictional drag was equal to zero. The value of 0.47 calculated by this study, and by Shea and Gray (1972), does not necessarily verify Riehl's theoretical results, since his relationship involves surface tangential stress which may not apply in regions above the boundary layer.

Malkus and Riehl (1960) have shown that a change in the equivalent potential temperature at the base of the eyewall is directly proportional to the associated change in surface pressure. Based on this finding, a relationship was sought between sudden increases in equivalent potential temperature (a "pulse") at the base of the eyewall and subsequent decreases in central surface pressure. An evaluation of the surface pressure changes associated with four rapidly deepening tropical cyclones indicated that a build-up in moist static energy (directly related to equivalent potential temperature) occurred just prior to a 48-h period of rapid deepening. Likewise, a subsequent drop in moist static energy during the 48-h deepening phase appeared to correlate with a later pressure rise in three of the four cases. However, the results of only four cases are not sufficient to establish a causality relationship.

The conclusive evidence needed to verify a relationship between moist static energy change and intensity change might be obtained through more extensive aircraft reconnaissance. It would be necessary to obtain complete low-level moist static energy data around the outside of the eyewall at closely spaced intervals. This would reduce the problem of having to determine an average low-level moist static energy value for the entire tropical cyclone based on only one or two observations at 700 mb. Also, if the observations were obtained at closely small time intervals, it would be less likely that a significant "pulse" would pass undetected.

In summary, a large amount of aircraft reconnaissance data from the vicinity of northwest Pacific tropical cyclones has been collected over the past 20 years by aircraft of the 54th Weather Reconnaissance Squadron. Although the observations are usually restricted to the 700 mb level, they can still provide useful information on the structure of tropical cyclones. The quality, but not quantity, of this data is on a par with the high density data collected by research aircraft in the Atlantic region. Also, there is some indication that significant changes in the

intensification trend of tropical cyclones are related to changes in the moist static energy of the low-level air. It may be possible to correlate the relationship during post-analysis, but the significant fluctuations that can occur are often too ambiguous to allow a forecaster to use moist static energy as an operational intensity forecast tool.

# LIST OF REFERENCES


Anthes, R. A., 1982: Tropical cyclones: Their evolution, structure and effects. American Meteorological Society, Boston, 208 pp.

Bell, G. J., and Tsui, Kar-Sing, 1973: Some typhoon soundings and their comparison with soundings in hurricanes. J. Applied Meteor., 9, 329-342.

Black, P. G., and R. A. Anthes, 1971: On the asymmetric structure of the tropical cyclone outflow layer. J. Atmos. Sci., 28, 1348-1366.

Charney, J. G., and A. Eliassen, 1964: On the growth of hurricane depressions. J. Atmos. Sci., 21, 68-75.

Dunnavan, G. M., 1981: Forecasting intense tropical cyclones using 700-mb equivalent potential temperature and central sea-level pressure. NAVOCEANCOMCEN/JTWC Tech Note 81-1, 12 pp.

Dunnavan, G. M., and J. W. Diercks, 1980: An analysis of super typhoon Tip (October 1979). Mon. Wea. Rev., 108, 1915-1923.

Frank, W. M., 1977: The structure and energetics of the tropical cyclone I. storm structure. Mon. Wea. Rev., 105, 119-1145.

Gray, W. M., 1965: Calculations of cumulus vertical draft velocities in hurricanes from aircraft observations. J. Appl. Meteor., 4, 463-474.

Gray, W. M., 1979a: Hurricanes: Their formation, structure, and likely role in the tropical circulation. Meteorology Over the Tropical Oceans, D. B. Shaw, Ed., Roy. Meteor. Soc., 155-218.

Gray, W. M., 1979b: Tropical cyclone intensity determination through upper-tropospheric aircraft reconnaissance. Bull. Amer. Meteor. Soc., 60, 1069-1074.

Hawkins, H. F., and D. T. Rubsam, 1968: Hurricane Hilda, 1964, II. Structure and budgets of the Hurricane on October 1, 1964. Mon. Wea. Rev., 96, 617-636.

Hawkins, H. F., and S. M. Imbembo, 1976: The structure of a small, intense hurricane, Inez 1966. Mon. Wea. Rev., 104, 418-442.

Henderson, R. S., 1980: WC-130 meteorological system and its utilization in operational weather reconnaissance. Air Weather Service Technical Report 80/02, 79 pp.

Holland, G. J., 1983: Tropical cyclones in the Australia/southwest Pacific region. Dept. of Atmos. Sci. Paper No. 363, Colo. State Univ., Ft. Collins CO, 264 pp.

Holliday, C. R., and A. H. Thompson, 1979: Climatological characteristics of rapidly intensifying typhoons. Mon. Wea. Rev., 107, 1022-1034.

Holton, J. R., 1979: An introduction to dynamic meteorology. Academic Press, New York, 391 pp.

Hughes, L. A., 1952: On the low-level wind structure of tropical storms. J. Meteor., 9, 422-428.

Joint Typhoon Warning Center, 1979-1982: Annual Typhoon Reports/Annual Tropical Cyclone Reports 1978-1981. Naval Oceanography Command Center/Joint Typhoon Warning Center, Guam, Mariana Islands.

Jordan, C. L., 1958: Estimation of surface central pressures in tropical cyclones from aircraft reconnaissance. Bull. Amer. Meteor. Soc., 39, 345-352.

Jordan, E. S., 1952: An observational study of the upper wind circulation around tropical storms. J. Meteor., 9, 340-346.

La Seur, N. E., and H. F. Hawkins, 1963: An analysis of hurricane Cleo (1958) based on data from reconnaissance aircraft. Mon. Wea. Rev., 91, 694-709.

Malkus, J. S., and H. Riehl, 1960: On the dynamics and energy transformation in steady-state hurricanes. Tellus, 12, 1-20.

Ramage, C. S., 1959: Hurricane development. J. Meteor., 16, 227-237.

Riehl, H., 1963: Some relationships between wind and thermal structure of steady state hurricanes. J. Atmos. Sci. 20, 276-287.

Riehl, H., 1970: Some aspects of cumulonimbus convection in relation to tropical weather disturbances Bull. Am. Meteor. Soc., 50, 587-595.

Riehl, H., 1975: Further studies on the origin of hurricanes. Dept. of Atmos. Sci. Paper No. 235, Colo. State Univ., Ft. Collins, Co., 22 pp.

Sadler, J. C., 1978: A role of the tropical upper tropospheric trough in early season typhoon development. Mon. Wea. Rev., 104, 1266-1278.

Shea, D. J., and W. M. Gray, 1972: The structure and dynamics of the hurricanes's inner core region. Atmospheric Sciences Paper No. 182, Colorado State University, 134 pp.

Shea, D. J., and W. M. Gray, 1973: The hurricane's inner core region. I. symmetric and asymmetric structure. J. Atmos. Sci., 30, 1544-1564.

Sheets, R. C., 1969: Some mean hurricane soundings. J. Appl. Meteor., 8, 134-146.

Sikora, C. R., 1976: An investigation of equivalent potential temperature as a measure of tropical cyclone intensity. FLEWEACEN TECH NOTE: JTWC 75-3, 12 pp.

Simpson, R. H., 1952: Exploring the eye of typhoon "Marge", 1951. Bull. Amer. Meteor. Soc., 7, 286-298.

Simpson, R. H., 1954: Structure of an immature hurricane. Bull. Amer. Meteor. Soc., 35, 335-350.

Simpson, R. H., and L. G. Starrett, 1955: Further studies of hurricane structure by aircraft reconnaissance. Bull. Amer. Meteor. Soc., 36, 459-468.

TSWA, Inc., 1945: Weather conditions on a flight across the tropical storm of October 19, 1944 while in northern Florida. Bull. Amer. Meteor. Soc., 26, 199-203.

Wexler, F. B., and H. Wood: Flight into the September 1944 hurricane off Cape Henry, Virginia. Bull. Amer. Meteor. Soc., 26, 153-159.

# INITIAL DISTRIBUTION LIST

| | | No. Copies |
|---|---|---|
| 1. | Defense Technical Information Center<br>Cameron Station<br>Alexandria, VA 22314 | 2 |
| 2. | Library, Code 0142<br>Naval Postgraduate School<br>Monterey, CA 93943 | 2 |
| 3. | Professor Robert J. Renard, Code 63Rd<br>Department of Meteorology<br>Naval Postgraduate School<br>Monterey, CA 93943 | 1 |
| 4. | Professor Christopher N. K. Mooers, Code 68Mr<br>Department of Oceanography<br>Naval Postgraduate School<br>Monterey, CA 93943 | 1 |
| 5. | Professor Russell L. Elsberry, Code 63Es<br>Department of Meteorology<br>Naval Postgraduate School<br>Monterey, CA 93943 | 2 |
| 6. | Dr. Johnny Chan, Code 63Ch<br>Department of Meteorology<br>Naval Postgraduate School<br>Monterey, CA 93943 | 1 |
| 7. | Professor William Gray<br>Department of Atmospheric Sciences<br>Colorado State University<br>Fort Collins, CO 80523 | 1 |
| 8. | Lt. George M. Dunnavan<br>5012 23 Av. S.E.<br>Lacey, WA 98125 | 3 |
| 9. | Director<br>Naval Oceanography Division<br>Naval Observatory<br>34th and Massachusetts Avenue NW<br>Washington, D.C. 20390 | 1 |
| 10. | Commander<br>Naval Oceanography Command<br>NSTL Station<br>Bay ST. Louis, MS 39522 | 1 |

11. Commanding Officer 1
Naval Oceanographic Office
NSTL Station
Bay St. Louis, MS 39522

12. Commanding Officer 1
Fleet Numerical Oceanography Center
Monterey, CA 93940

13. Commanding Officer 1
Naval Ocean Research and Development
Activity
NSTL Station
Bay ST. Louis, MS 39522

14. Commanding Officer 1
Naval Environmental Prediction Research
Facility
Monterey, CA 93940

15. Dr. Ted Tsui 1
Naval Environmental Prediction Research
Facility
Monterey, CA 93940

16. Chairman, Oceanography Department 1
U.S. Naval Academy
Annapolis, MD 21402

17. Chief of Naval Research 1
800 N. Quincy Street
Arlington, VA 22217

18. Office of Naval Research (Code 480) 1
Naval Ocean Research and Development
Activity
NSTL Station
Bay ST. Louis, MS 39522

19. Commander 1
Oceanographic Systems Pacific
Box 1390
Pearl Harbor, HI 96860

20. Commander 1
Air Weather Service
Scott Air Force Base, IL 62225

21. Director 1
Joint Typhoon Warning Center
COMNAVMARIANAS Box 17
Fleet Post Office
San Francisco, CA 96630

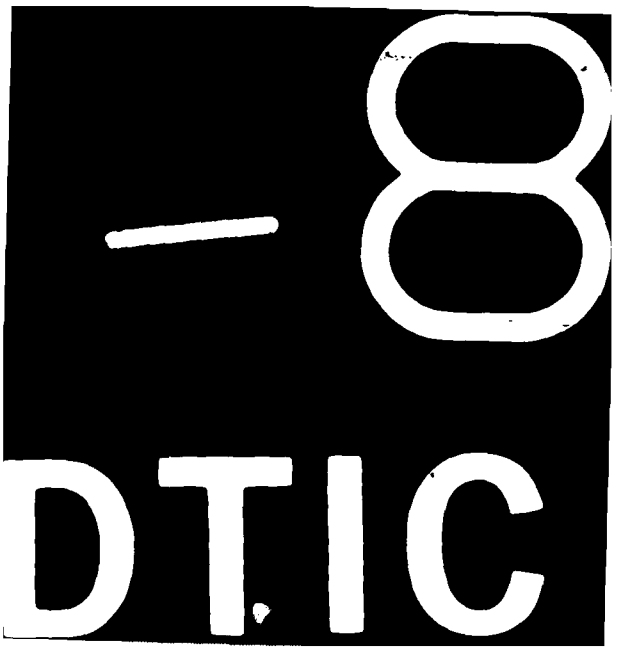
-8
DTIC